

UNIVERSITY OF MINNESOTA  
**ST. ANTHONY FALLS LABORATORY**  
Engineering, Environmental and Geophysical Fluid Dynamics

**Project Report No. 525**

**A flow and temperature model for the Vermillion River,  
Part II: Response to surface runoff inputs**

by

William Herb and Heinz Stefan



Prepared for

**Minnesota Pollution Control Agency**  
St. Paul, Minnesota

December 2008  
**Minneapolis, Minnesota**

The University of Minnesota is committed to the policy that all persons shall have equal access to its programs, facilities, and employment without regard to race, religion, color, sex, national origin, handicap, age or veteran status.

## Abstract

Stream temperature and stream flow are crucial physical parameters for aquatic habitat preservation in rivers and streams. Water temperature is particularly important in coldwater stream systems that support trout. Summer base (low) flow conditions with high water temperatures can be very detrimental to trout habitat. Surface runoff from rainfall events can lead to increases in stream temperature, particularly in developed (urban) watersheds. To better understand the interactions between stream temperature, land use, and climate, a stream thermal impact model has been developed for the Vermillion River, Minnesota.

The model includes an unsteady streamflow and a water temperature model for the main stem of the Vermillion from Dodd Avenue to Goodwin Avenue and a number of tributaries, including South Branch, South Creek, North Creek, and Middle Creek. The EPD-riv1 package was used to simulate stream flow, including distributed groundwater inputs. A stream temperature model has been assembled based on previous work at SAFL. The stream temperature model uses flow and flow area from the flow solver, along with observed climate data to calculate surface heat transfer. The assembled flow and temperature model for the Vermillion River has been calibrated for baseflow conditions.

Surface runoff inputs to the Vermillion River were simulated using a GIS-based land heat contribution model, which was developed and run by Applied Ecological Services. Surface runoff volume and temperature time series were simulated for a ½" rainfall event in 35 sub-watersheds. Simulated runoff volumes and temperatures from the 35 sub-watersheds were used as input to the stream flow and temperature model, to simulate the hydraulic and thermal response of the Vermillion to runoff from the ½" rainfall event. Stream temperature increases due to surface runoff were found to be highest (1-4°C) in smaller, upstream tributaries of South Creek and North Creek, and lowest in lower portions of the main stem and South Branch (< 1 °C). Overall, the stream temperature response to multiple surface inflows was found to be quite complex.

The coupled surface runoff and stream temperature model was used to examine several future urban development scenarios for the South Creek watershed and several possible strategies for mitigation of thermal impact downstream from the development. The model was able to resolve the stream temperature impact of a single 200 acre development. Full development in the upper South Creek watershed gave stream temperature increases over present conditions ranging from 3.8°C in small tributaries to South Creek to less than 0.1°C at the main stem of the Vermillion River near Empire. Downstream mitigation of thermal impacts from surface runoff was found to be ineffective, because the downstream watersheds were relatively undeveloped, and much of the thermal impact from upstream was lost by atmospheric heat transfer and dilution by the time the flow reached the sub-watersheds downstream. Adding channel shading to downstream stream reaches did not reduce the magnitude of the thermal impacts from upstream surface runoff, but did reduce maximum stream temperatures during dry weather periods, as would be expected.

## Table of Contents

1. Introduction.....	5
2. Model Description .....	6
3. Baseflow Scenarios for the Vermillion River.....	7
4. Surface Runoff Input Specification .....	9
5. Hydro-thermal Response of a Stream Reach to Surface Runoff Inputs .....	15
6. Model Validation .....	19
7. The Combined Response of the Vermillion River to the Design Storm.....	25
8. Effects of Land Development and Mitigation Scenarios.....	38
9. Summary of Results.....	47
Acknowledgments.....	49
References.....	50
Appendix I. Analytic model for temperature decay of surface runoff.....	51
Appendix II. Design storm.....	59

# 1. Introduction

Water temperature and stream flow are important parameters for aquatic habitat preservation in river and stream systems. Water temperature is particularly important for coldwater stream systems that support trout. Summer base flow conditions (low flows) and high water temperatures can be critical for maintaining trout habitat. Surface runoff from rainfall can increase stream temperature, particularly in developed (urban) watersheds. To better understand the interactions between stream temperature, land use, and climate, an unsteady stream flow and temperature model has been developed for the Vermillion River. This river is at the southern fringes of the Twin Cities metropolitan area (Figure 1.1) and has a world-class brown trout fishery.

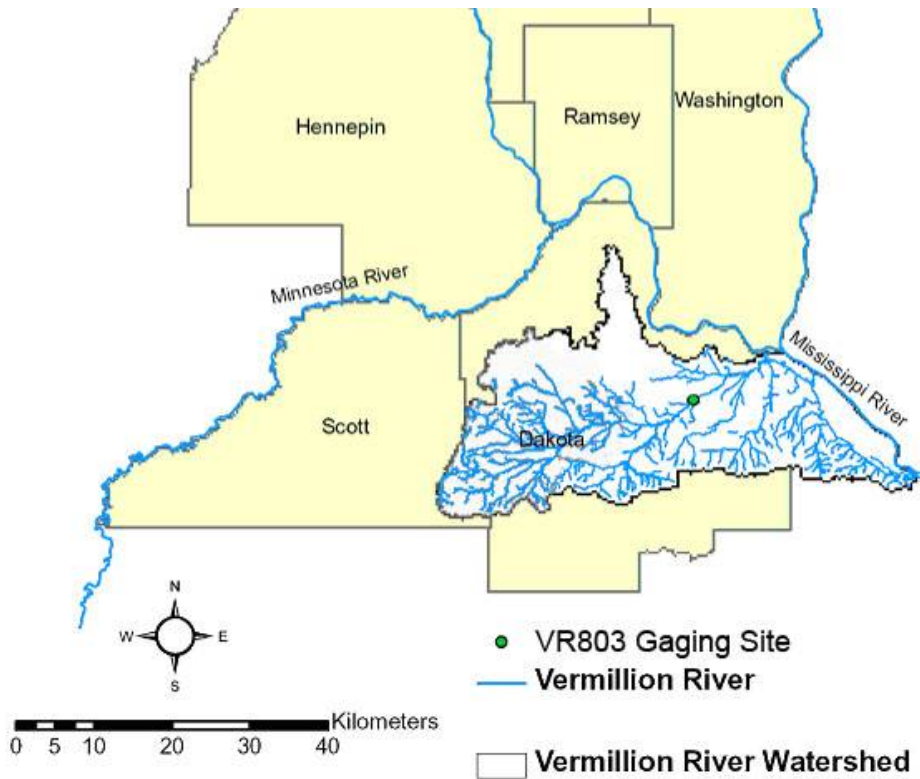


Figure 1.1. The Vermillion River watershed in Scott and Dakota counties. The study area includes the Vermillion River main stem and major tributaries upstream of the VR803 station, near the town of Vermillion, MN.

The stream flow and temperature model is designed to simulate the response of the Vermillion River to surface runoff events, however, the model can be run for continuous analysis of several months. Groundwater inputs to the river (flow per unit length and temperature) are included, and are an important part of the flow and temperature simulations. In addition to detailed temperature and flow time series, the model provides broad scale characterizations of heat transport in the Vermillion River, including the relative importance of groundwater temperature, atmospheric heat transfer, and surface water inputs in determining stream temperature. The stream temperature model can therefore be used as a tool to determine what management practices (e.g. stormwater BMPs, bank shading, groundwater conservation) are best to maintain

cold water temperatures for trout habitat. This report (Part II) describes the response of the river to surface runoff inputs. The model formulation and calibration for baseflow conditions was described previously in Part I, SAFL Project Report No. 517. For convenience, some information given in Part I is repeated in this report.

## 2. Model Description

The stream flow and temperature model includes the main stem of the Vermillion River from Dodd Avenue to Goodwin Avenue and a number of tributaries, including South Branch, South Creek, North Creek, and Middle Creek (Figure 2.1). The EPD-riv1 package (US EPA 2005) was used to simulate unsteady stream flow, including distributed groundwater inputs. A stream temperature model was developed and assembled based on previous work at SAFL (Sinokrot and Stefan 1993,1994). The stream temperature model uses flow rates and flow areas from the flow solver, along with observed climate data to calculate surface heat transfer (Figure 2.2). Stream flow is simulated at 1 to 5 minute time steps, while stream temperature is simulated at 15 minute to 1 hour time steps, using observed climate data as the primary input. Groundwater inflows are an important component of both the flow and temperature model. For the Vermillion River, groundwater inflow rates were estimated from flow gaging sites, while groundwater temperatures were estimated by calibrating the stream temperature model against measured stream temperatures. The land cover heat contribution model, a GIS-based runoff model developed by Applied Ecological Services, Inc. (AES 2008), supplies surface runoff volumes and temperatures for individual rainfall events, which are used as an input to the stream flow and temperature models (Figure 2.2)

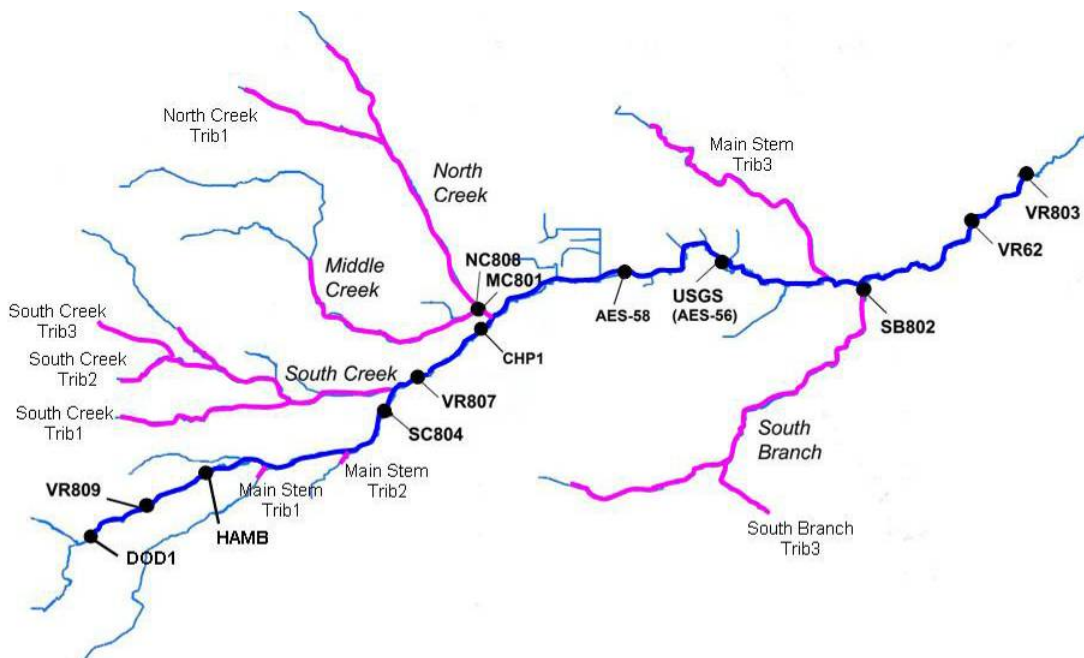


Figure 2.1. Extent of the flow and temperature model for the Vermillion River main stem (dark blue line) and tributaries (pink lines). The upstream end (DOD1) is Dodd Boulevard, while the downstream end (VR803) is Goodwin Avenue. Main stem Trib1 and Trib2 are specified flow

input points to the main stem model, but these tributaries are not modeled separately. Main stem Trib3 is modeled separately.

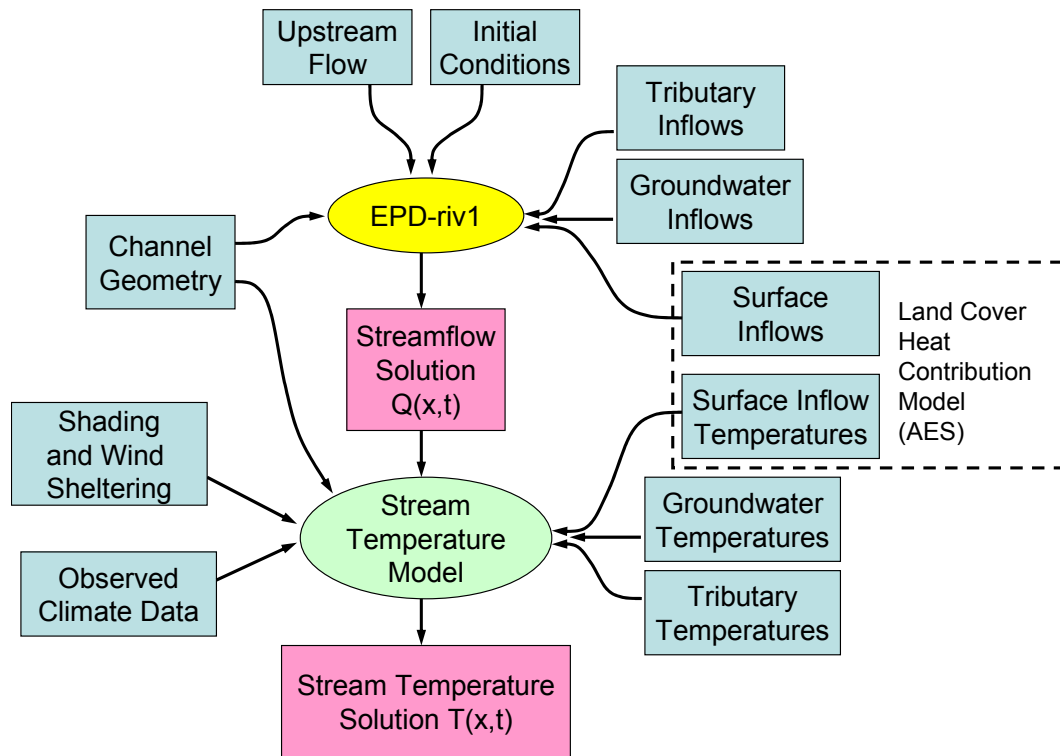


Figure 2.2. Flow chart summarizing the input data and simulation results for the flow and temperature solvers used in this study.

### 3. Baseflow Scenarios for the Vermillion River

Two baseflow scenarios were created for the Vermillion River main stem and tributaries. The first baseflow scenario, a mid-summer baseflow for the period August 9 to September 8, 2006, was created from observed 2006 flow data and used for calibration of the stream temperature model (Herb and Stefan 2008b). The main stem baseflow was set after analysis of 30 years of flow data at the Empire USGS gaging station. Flows at other points in the main stem and tributaries were set to be a fraction of the flow at the USGS station, based on summer monthly-averaged flows at six other gaging stations (Herb and Stefan 2008a). Groundwater inflows were uniformly distributed over three reaches of the main stem (Table 3.1), based on monthly-averaged flow differences between gaging stations (Herb and Stefan 2008b). Effluent from the Empire WWTP to the main stem was set based on plant influent data supplied by the Met Council. Groundwater inputs to the tributaries were estimated based on available gaging stations and point flow measurements taken by the Dakota County SWCD (Herb and Stefan 2008b).

Table 3.2 summarized the specified upstream flow inputs and distributed groundwater flows for each stream reach. In most cases, there was no flow gage at the upstream end of the tributary. A low value for the upstream input was assumed (0.25 cfs) and increased if necessary to enable unsteady flow analysis of simulated stormwater inputs. Groundwater inputs to the model were adjusted to achieve a match of known downstream flow values with modeled flows, or to give agreement in simulated and observed stream temperatures at the downstream location. For the case of, e.g., South Creek Trib1, groundwater inputs needed to be concentrated near the downstream end of the stream reach to produce the low observed stream temperature.

The second baseflow scenario is similar to the first scenario, except that the Empire WWTP effluent is omitted. This baseflow scenario is intended to represent flow conditions for present and future conditions, because the Empire WWTP effluent was diverted in a pipeline to the Mississippi River in Fall 2007. This second baseflow scenario was used as an initial condition for all surface runoff thermal impact analyses described in this report. A longitudinal distribution of stream flow under the two baseflow scenarios (with and without the Empire effluent) is given in Figure 3.1. The step increases due to tributaries and upward trends due to distributed groundwater inputs are clearly shown.

Table 3.1. Specified groundwater flow inputs for the main stem of the Vermillion River for the August /September 2006 baseflow scenario. RS 32.4 is 0.7 miles downstream of Hamburg Avenue.

Reach	Length (km)	Groundwater Input (cfs)	Groundwater Input Rate (cfs/mile)
DOD1 to VR809	2.56	0.0	0.0
VR809 to RS 32.4	3.60	1.4	0.39
RS 32.4 to VR807	10.32	0.0	0.0
VR807 to USGS	14.56	11.0	0.75
USGS to VR803	15.44	9.4	0.61

Table 3.2. Summary of specified upstream inputs and distributed groundwater flows for each tributary reach. The location of each tributary is shown in Figure 2.1.

Reach	Length (km)	Upstream Baseflow Input (cfs)	Groundwater Input (cfs)
Main Stem Trib1	10.7	0.25	0.25
Middle Creek	5.6	0.5	0.5
North Creek	7.1	0.5	5.25
North Creek Trib1	2.9	0.5	0.5
South Branch	14.4	0.5	5.1
South Branch Trib1	2.5	0.5	0.5
South Creek	8.8	0.25	5.6
South Creek Trib1	5.7	0.5	1.75
South Creek Trib2	2.9	0.25	0.4
South Creek Trib3	1.6	0.25	0.4



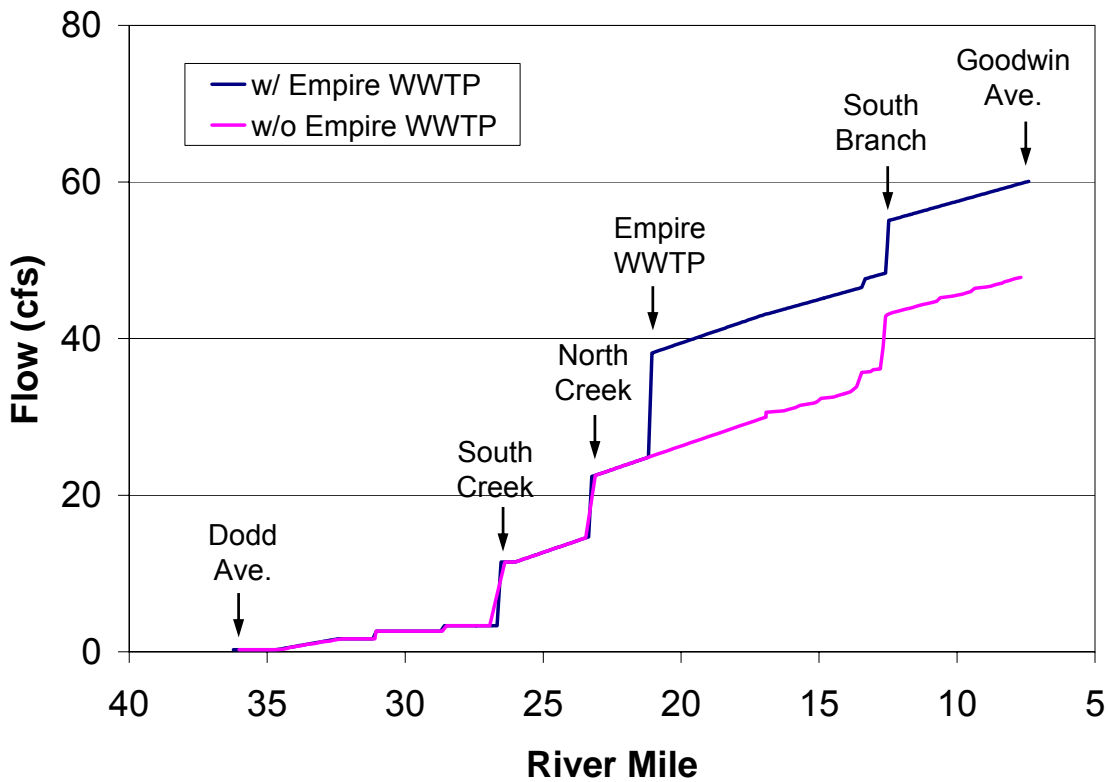


Figure 3.1. Simulated longitudinal distribution of flow in the main stem of the Vermillion River on August 1, 2005.

#### 4. Surface Runoff Input Specification

Surface runoff inputs for several storm events were supplied for this project by Applied Ecological Services, Inc. (AES). While SAFL has a runoff-temperature model applicable to small areas of land (e.g. 10 – 100 acres), it is currently not applicable at the watershed level. To enable watershed level simulation of runoff and runoff temperature, AES developed a GIS-based model to estimate runoff and runoff temperature at the watershed level (AES 2008): Thirteen hydro-thermal land uses (pavements, rooftops, lawn, cropland, wetlands, etc.) are mapped onto the watershed at 10 x 10 m resolution (Figure 4.1, upper panel). Runoff temperatures are specified for each land use for a particular storm by the SAFL runoff temperature model, summarized in Table 4.1 (Herb et al. 2007). Runoff volumes for the storm are calculated for each 10 x 10 m pixel using a curve number algorithm. An example of the resulting heat export from each 10 x 10m pixel is shown in Figure 4.1 (lower panel), where heat export ( $h$ ) is defined as (Herb et al. 2007):

$$h = \rho C_p Q (T_{ro} - T_{ref}) \quad (4.1)$$

where  $\rho$  and  $C_p$  are the density and specific heat of water,  $Q$  is the runoff flow rate (e.g.  $m^3/s$ ),  $T_{ro}$  is the runoff temperature, and  $T_{ref}$  is the reference temperature. The runoff volumes and

temperatures are combined and routed through the watershed to the pour points using a travel time algorithm, based on flow velocity over various land covers. 35 sub-watersheds are defined in the GIS runoff model (Figure 4.2), which route runoff to 35 pour points (input points to the Vermillion River system stream flow and temperature model). An equilibrium temperature relationship is used to estimate a runoff temperature decay over distance and time (Appendix I); this algorithm provides some adjustment of runoff temperatures to specified climate after the storm event.

The algorithms used for the routing of surface runoff over each sub-watershed take into account surface topography, but do not include storm sewers. As a result, surface runoff inputs from developed areas such as downtown Farmington are not necessarily routed to the actual input point to the river.

Examples of surface runoff inputs for the ½” design storm are given in Figure 4.3. The simulated runoff responses lasted up to 17 hours; the average was 6.8 hours. Table 4.2 summarizes the duration, volume, temperature, and heat export for the 35 sub-watersheds.

Table 4.1. Simulated runoff temperatures and heat exports for the ½” design storm event.

<b>Land Use</b>	<b>Average Runoff Temp (°C)</b>	<b>Heat Export<sup>1</sup> (kJ/m<sup>2</sup>)</b>
Commercial Roof	25.98	420.8
Concrete	25.52	396.7
Asphalt	25.15	377.5
Bare Soil	25.66	258.5
Residential Roof	20.31	123.6
Short Grass	21.47	118.9
Corn	21.37	114.2
Tall Grass	21.46	113.6
Forest	20.9	96.4
Pond	23.3	159.1
Vegetated Pond	19.4	-19.9
Lake	25.6	245.7
Wetland Complex	20.0	58.0
1. Reference Temp = 18 °C		

Table 4.2. Summary of surface runoff inputs from the 35 sub-watersheds in the AES model for the ½” design storm event. Heat export was calculated using a reference temperature of 18 °C.

Sub-watershed	Duration (hours)	Max Runoff Rate (cfs)	Total Runoff Volume (m <sup>3</sup> )	Ave. Runoff Temp (°C)	Total Heat Export (GJ)
SUB_01	3	2.0	264.3	24.9	7.6
SUB_02	1.75	0.7	75.2	22.8	1.5
SUB_03	2.75	2.6	292.8	22.4	5.4
SUB_04	3.25	2.2	390.3	23.8	9.6
SUB_05	3.75	0.8	129.3	23.5	3.0
SUB_06	6.75	2.7	512.8	22.6	9.9
SUB_07	6.75	2.6	340.4	22.3	6.2
SUB_08	8.25	1.4	434.0	22.2	7.7
SUB_09	11.75	2.2	538.9	22.5	10.1
SUB_10	4	1.2	145.7	23.2	3.2
SUB_11	6	31.7	3278.8	24.0	82.4
SUB_12	5	2.7	412.5	23.8	10.0
SUB_13	8.5	1.2	306.9	22.1	5.3
SUB_14	11	8.3	2812.1	22.8	57.1
SUB_15	4.75	3.8	632.3	24.6	17.5
SUB_16	11.25	4.9	1910.0	24.0	48.5
SUB_17	6.5	9.5	1391.5	23.5	32.2
SUB_18	11	10.3	4435.7	23.5	102.9
SUB_19	4	1.7	310.6	23.4	7.0
SUB_20	6	18.5	3331.4	24.1	85.5
SUB_21	8.25	6.4	1360.9	23.9	33.8
SUB_22	5	14.1	1420.7	23.8	34.8
SUB_23	6.75	9.9	1837.8	23.6	43.3
SUB_24	7.5	0.6	115.9	24.0	2.9
SUB_25	6.5	25.6	2715.3	24.1	69.5
SUB_26	5.75	2.0	290.4	23.0	6.1
SUB_27	3.25	11.3	1796.6	24.2	46.5
SUB_28	5	15.5	3294.4	24.4	88.7
SUB_29	4.25	7.3	1133.9	24.1	28.9
SUB_30	8	2.1	615.9	22.5	11.5
SUB_31	7.75	2.7	820.4	23.1	17.4
SUB_32	11.5	4.8	1650.0	22.8	33.3
SUB_33	17	10.2	1891.2	22.2	49.3
SUB_34	13.75	12.6	3922.2	22.8	81.3
SUB_35	4.25	6.4	634.1	23.3	14.0

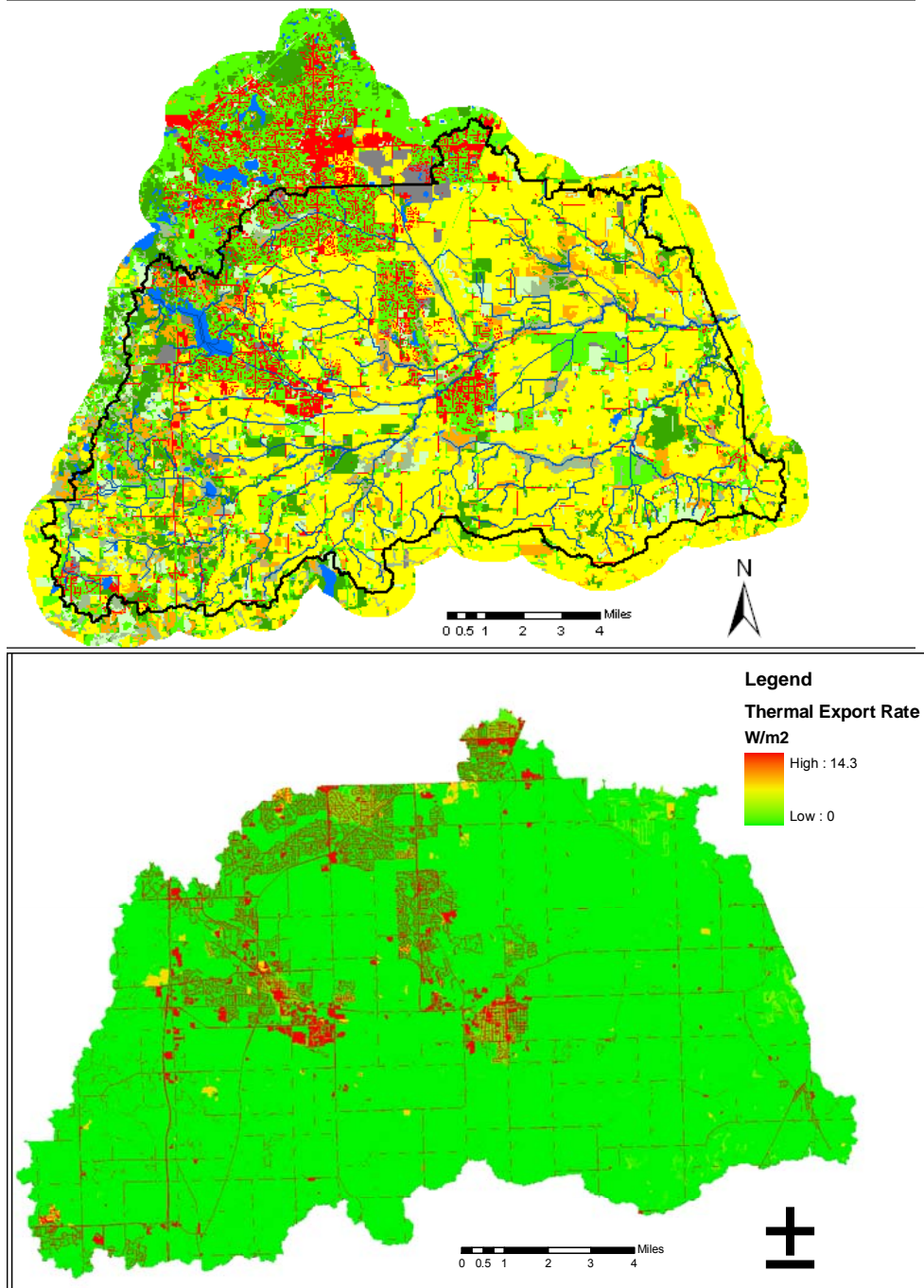


Figure 4.1. GIS map of the hydro-thermal land uses specified on 10 x 10 m resolution for the Vermillion River watershed (upper panel), and the calculated heat export rate for each pixel for the design storm (lower panel). Images supplied by AES, Inc.

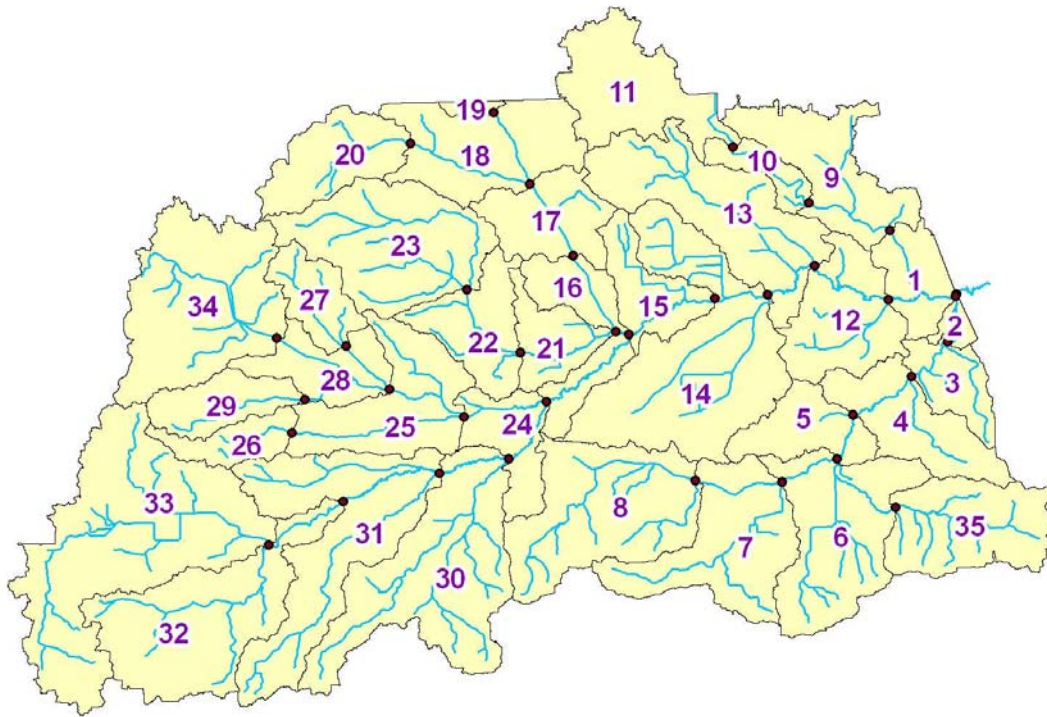


Figure 4.2. Sub-watersheds defined in the thermal impact model, with the pour points shown as black dots. The pour points are the points at which surface runoff is introduced into the stream flow and temperature model.

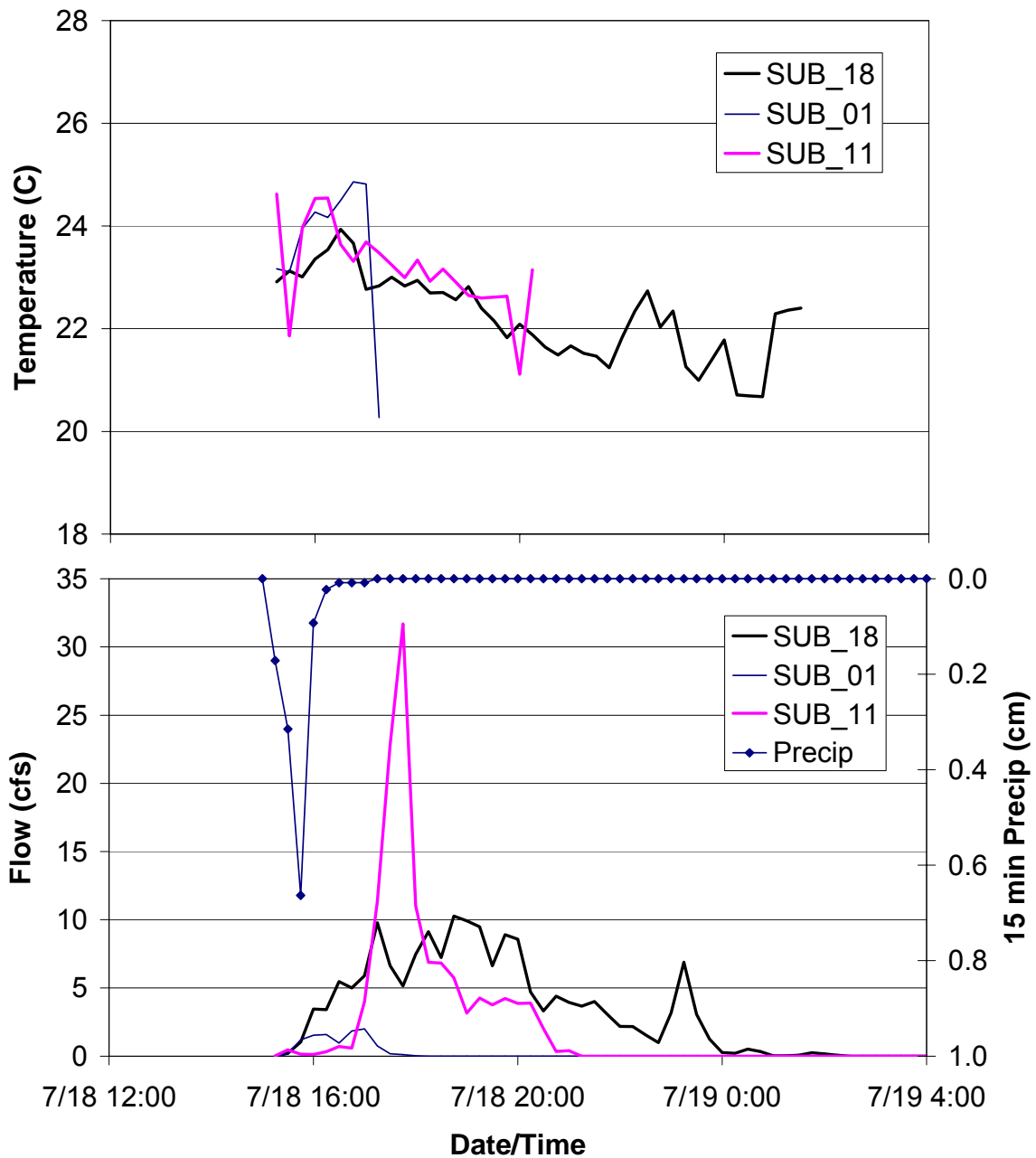


Figure 4.3. Sub-watershed runoff rates and temperatures from the AES thermal loading model for three sub-watersheds, using the ½” design storm as input. Sub-watershed 18 had the highest runoff volume (4400 m<sup>3</sup>) and the highest total heat export (102 GJ), sub-watershed 11 had the highest peak runoff rate (31.7 cfs), and sub-watershed 1 had the highest average runoff temperature (24.9 °C).

## 5. Hydro-thermal Response of a Stream Reach to Surface Runoff Inputs

The combined response of the Vermillion River to all 35 sub-watershed inputs is quite complex. It is therefore useful to first examine the flow and temperature response of a single stream reach to a single surface runoff input. Two individual reaches will be examined in this section: a smaller reach (South Creek) and a larger reach (main stem, downstream from the confluence with North Creek). Simulations were performed for South Creek in response to surface runoff from sub-watershed #27, and for the main stem in response to surface runoff input from sub-watershed #16. Both surface runoff inputs were provided by AES for the design storm (Appendix II).

The flow responses are shown in Figure 5.1. In both cases, the surface runoff input pulses remain essentially intact as they travel downstream. For the smaller reach (South Creek), the surface runoff input is clearly a larger fraction of the baseflow compared to the main stem. Moderate smoothing of the pulses with distance is likely due to a combination of friction effects and numerical dispersion. The overall increase in the baseflow with distance downstream is due to groundwater inputs.

The temperature change due to surface runoff inputs depends on both the flow and temperature of the input and the flow and temperature of the receiving stream. The stream temperature change at the input point ( $\Delta T$ ) can be calculated as:

$$\Delta T = \frac{Q_{ro}(T_{ro} - T_s)}{(Q_s + Q_{ro})} \quad (5.1)$$

where  $Q_{ro}$  and  $T_{ro}$  are the flow rate and temperature of the inflow, and  $Q_s$  and  $T_s$  are the flow and temperature of the stream just upstream of the input. For surface runoff inputs of a given rate and temperature, it is expected that inputs into low flow upstream tributaries will create larger temperature changes than the same inputs into higher flow reaches, e.g. the main stem. This expectation is confirmed in the stream temperature simulation results for South Creek and the main stem: South Creek temperature increased about 6 °C due to the input from sub-watershed #27, while the main stem temperature increased only about 1 °C due to input from sub-watershed #16 (Figure 5.2).

Since stream temperature is responding to both heat exchange with the atmosphere and heat inputs from surface runoff, the temperature response to surface inputs can be seen more clearly when plotted as a temperature difference, i.e. (stream temperature with surface inputs) - (stream temperature without surface inputs). This differential temperature has been plotted as a function of time and distance for the South Creek and main stem reaches in Figure 5.3. The stream temperature changes show marked decay with distance downstream and time. As the warmer water travels downstream, heat exchange with the atmosphere tends to remove excess heat and bring the stream temperature back to its original value. Input of cool groundwater dilutes the warmer water in the stream, and further reduces the temperature of the pulse as it travels downstream.

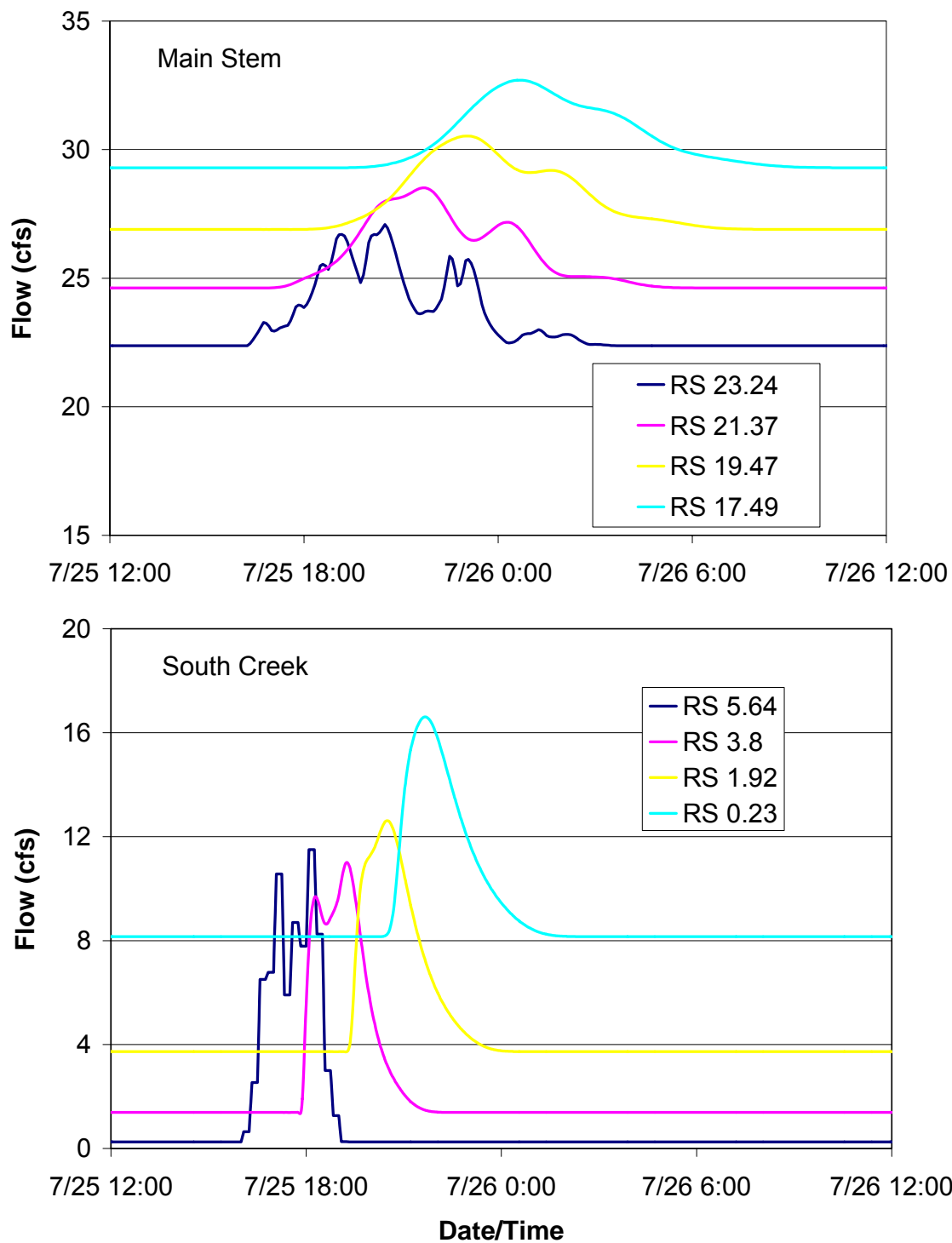


Figure 5.1. Simulated stream flow versus time at four stations in South Creek (lower panel) and the main stem (upper panel).



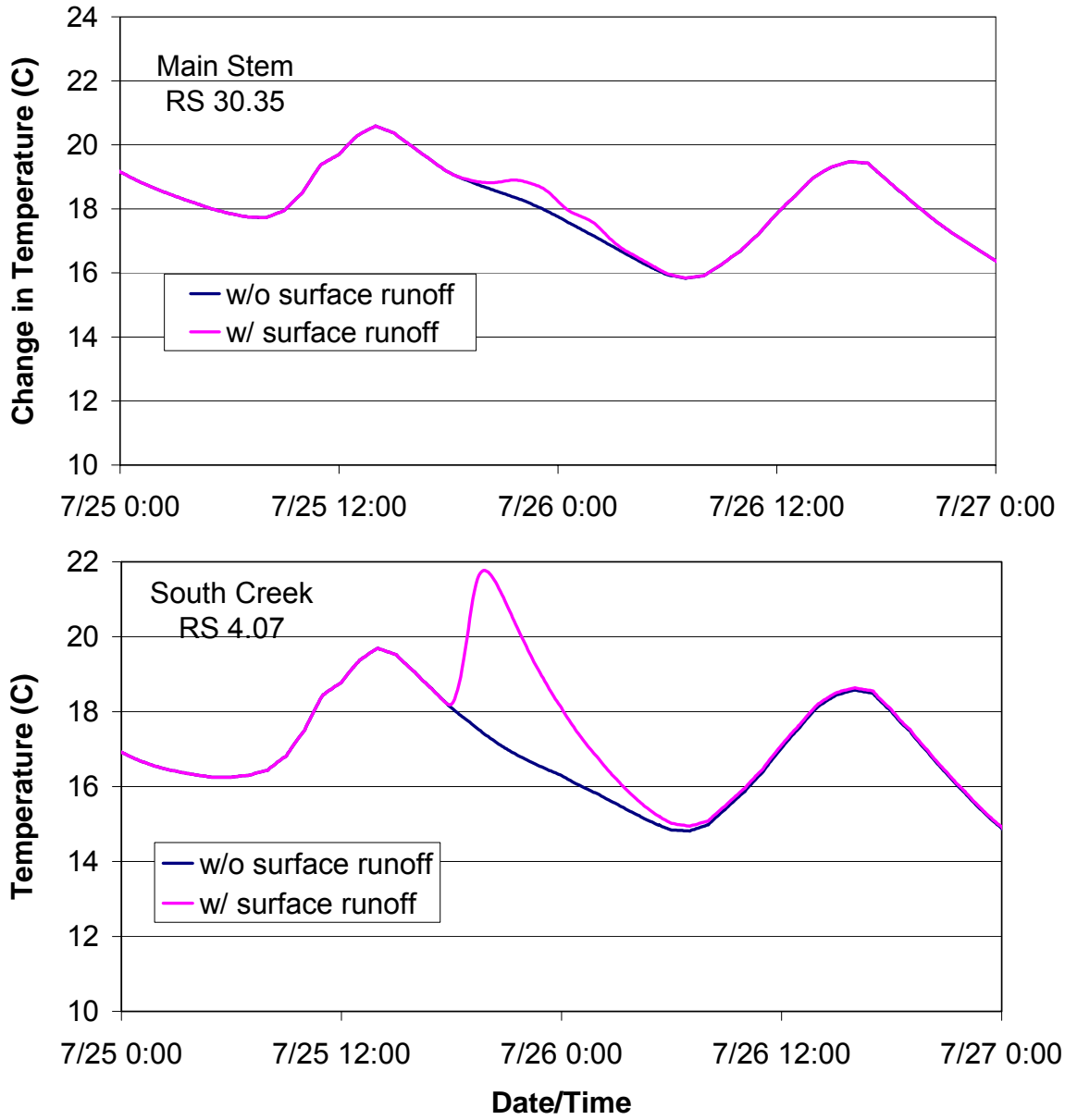


Figure 5.2. Simulated stream temperature versus time at stations in the Vermillion River main stem (upper panel) and in South Creek (lower panel) with and without surface runoff inputs.

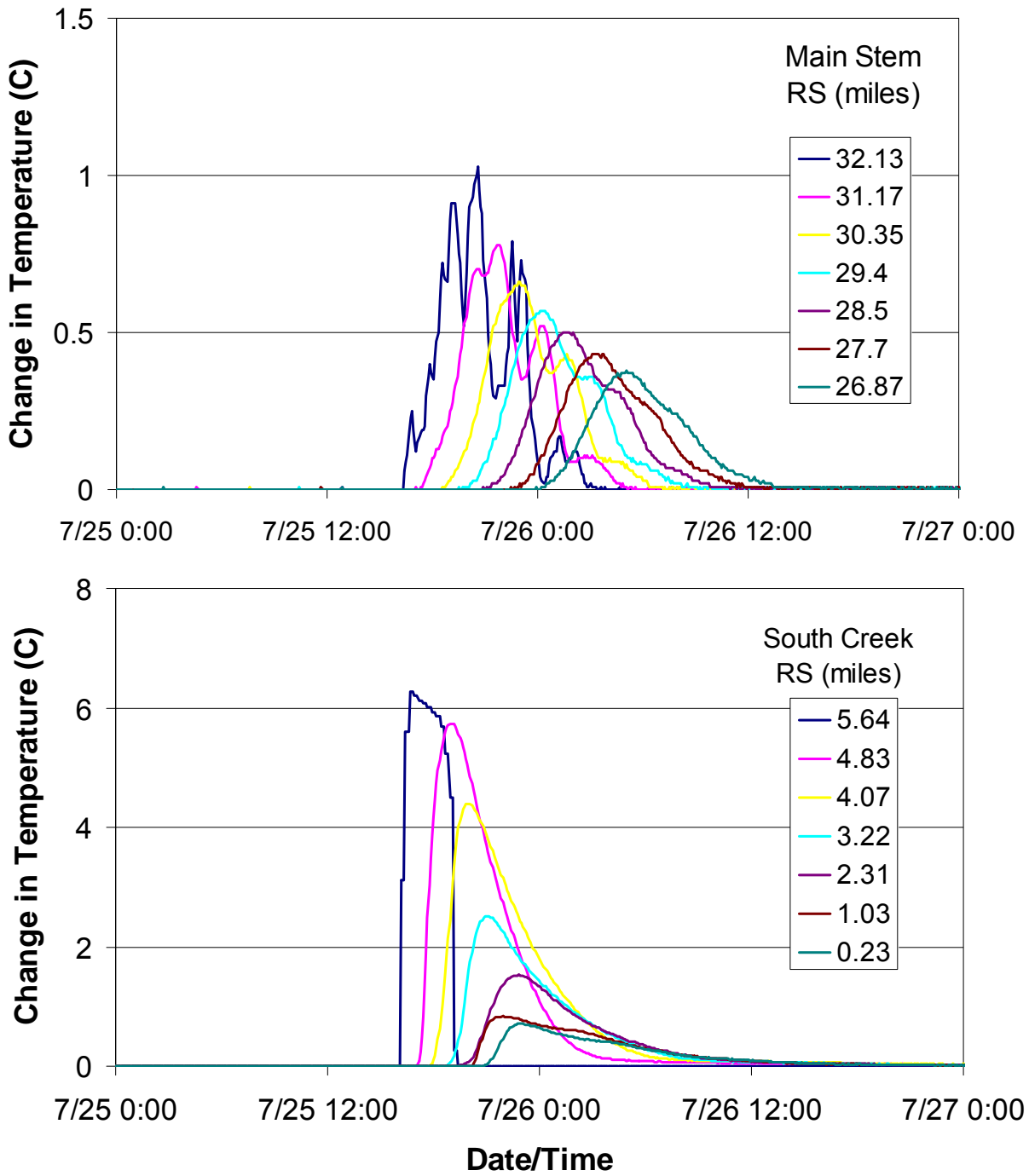


Figure 5.3. Simulated stream temperature difference due to surface runoff input versus time at stations in the main stem (upper panel) and South Creek (lower panel). Stream temperature difference is the incremental change in stream temperature due to a surface runoff input.

## 6. Model Validation

The stream temperature model was previously validated for baseflow conditions for a month long period in 2006 (Herb and Stefan 2008b) with a 1 to 2 °C RMSE between simulated and observed stream temperatures. To test the coupled thermal impact model, an observed rainfall event on July 19, 2006 was chosen, mainly because it produced observable flow and temperature responses at a number of points in the Vermillion River basin, and similar precipitation data were obtained from the University of Minnesota Rosemount Research and Outreach Center and the Empire WWTP (Figure 6.1). The rainfall totals at Rosemount and Empire were 3.0 and 2.4 cm, respectively. The runoff simulations were run using the Empire WWTP precipitation data, as it is more centrally located in the watershed.

The validation was performed for a sub-set of the complete watershed, encompassing the sub-watersheds for South Creek and the main stem downstream of the South Creek confluence to the Empire WWTP (Figure 6.2). This portion of the watershed was chosen because it is under intense urban development and includes important trout habitat. Simulated surface runoff from the sub-watersheds shown in yellow in Figure 6.2 was applied to the stream temperature model. Observed stream flows and temperatures were used as the upstream boundary condition at station SC804.

Surface runoff temperatures were simulated for 13 land use types using the SAFL runoff temperature model, and supplied to AES as input to the land cover heat contribution model. In general, simulated runoff temperatures for the July 19 storm (Table 6.1) were lower than those for the design storm (Table 4.1), because the July 19 storm occurs in the morning, when surface temperatures are lower. As with the design storm, the AES model was used to generate time series of surface runoff rates and temperatures at the pour points.

The simulated and observed streamflow response at points in South Creek and the main stem are shown in Figure 6.3. At the South Creek station, the magnitude and duration of the streamflow peak due to the storm are quite well reproduced. The timing of the observed and simulated flow peaks differ by about 8 hours. Some of this discrepancy can be attributed to the methods used to estimate the observed flow peak. There is no flow gaging station at the lower end of South Creek, flow was estimated by taking the difference between readings at stations VR807 and SC804, which are about 1.2 miles apart (Figure 6.2). The timing of the observed and simulated flow peaks at the VR807 station have better agreement (within 1.5 hours). The increase in observed baseflow, from before to after the storm, is not reproduced by the model, since no attempt is made in the model to specify time varying groundwater inflow rates. The only model parameter calibration that was done for the July 19 storm was adjustment of the curve numbers in the land cover heat contribution model to better match observed stream flows in the main stem.

The simulated and observed stream temperature responses to the July 19, 2006 storm are shown in Figures 6.4 and 6.5. In South Creek, the model under-predicts the observed increase in stream temperature due to surface runoff (Figure 6.4). Because of the uncertainty in the flow response, the discrepancy in the temperature response may be due to errors in the runoff temperatures, runoff volumes, or in the assumed baseflow conditions prior to the storm. Better flow data in

South Creek are needed to reproduce observed stream temperature fluctuations. Stream temperature fluctuations in the main stem were reproduced fairly well (Figure 6.5) at the VR807 and BSC2 sites. A relatively sharp stream temperature increase is evident at the CHP1 site, which may be attributed to storm sewer inflows from downtown Farmington. The model does not reproduce this peak, because storm sewers are not included in the land cover heat contribution model. The overall addition of heat at this location appears to be reproduced by the model fairly well, however.

Table 6.1. Simulated runoff temperatures and heat exports for the July 19, 2006 rainfall event.

<b>Land Use</b>	<b>Average Runoff Temp (C)</b>	<b>Heat Export <sup>1</sup> (kJ/m<sup>2</sup>)</b>
Asphalt	20.59	254.6
Bare Soil	22.34	329.3
Com Roof	19.30	128.6
Concrete	21.12	305.8
Corn	20.19	166.3
Forest	20.7	205.3
Lake	27.7	313.3
Pond	23.8	552.2
Res Roof	18.32	31.3
Short Grass	21.07	235.0
Tall Grass	20.83	211.1
Vegetated Pond	19.9	137.5
Wetland Complex	21.5	232.8
1. Reference Temp = 18 °C		

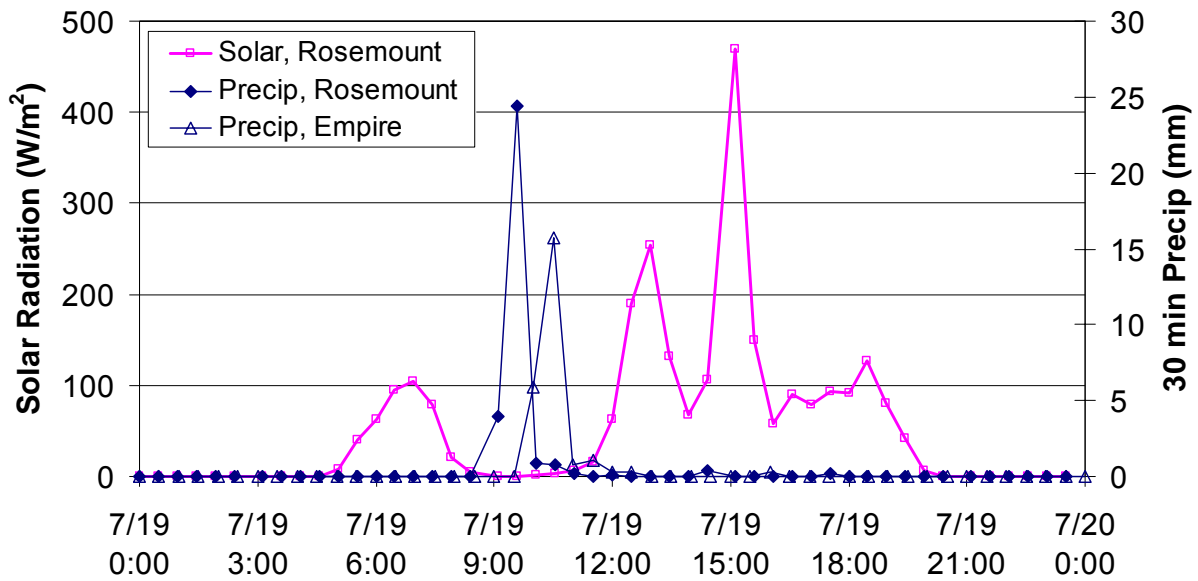


Figure 6.1. 30-minute time series of precipitation and solar radiation data from the University of Minnesota Rosemount Research and Outreach Center and Empire WWTP.

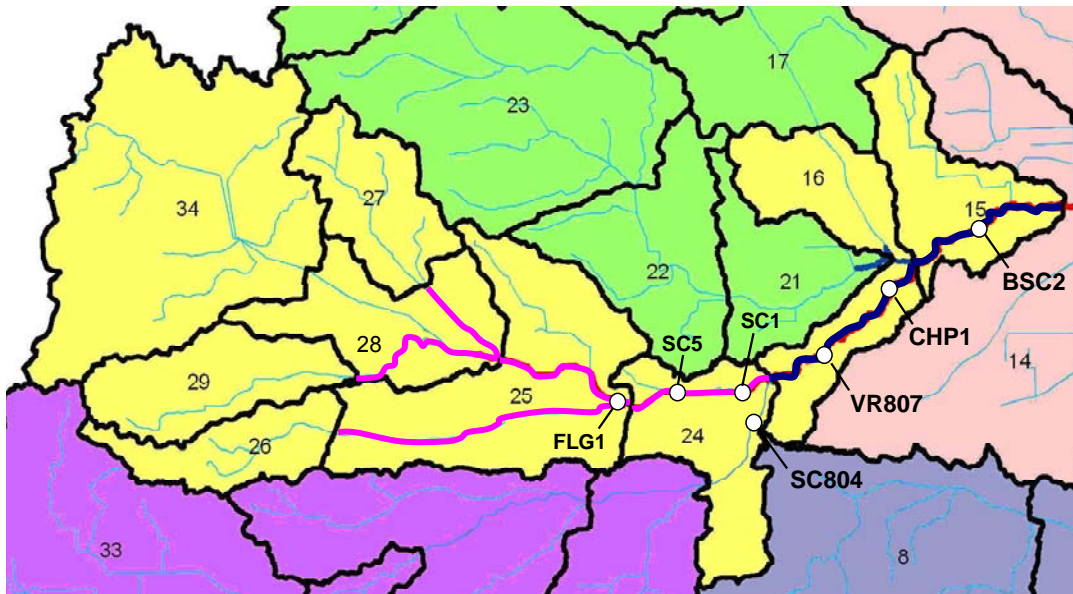


Figure 6.2. The portion of the Vermillion River watershed used for the calibration/validation study (in yellow), including South Creek reaches (highlighted in pink) and the main stem from South Creek to Empire (highlighted in dark blue). The stream temperature and flow measurement points used for calibration/validation are also shown.

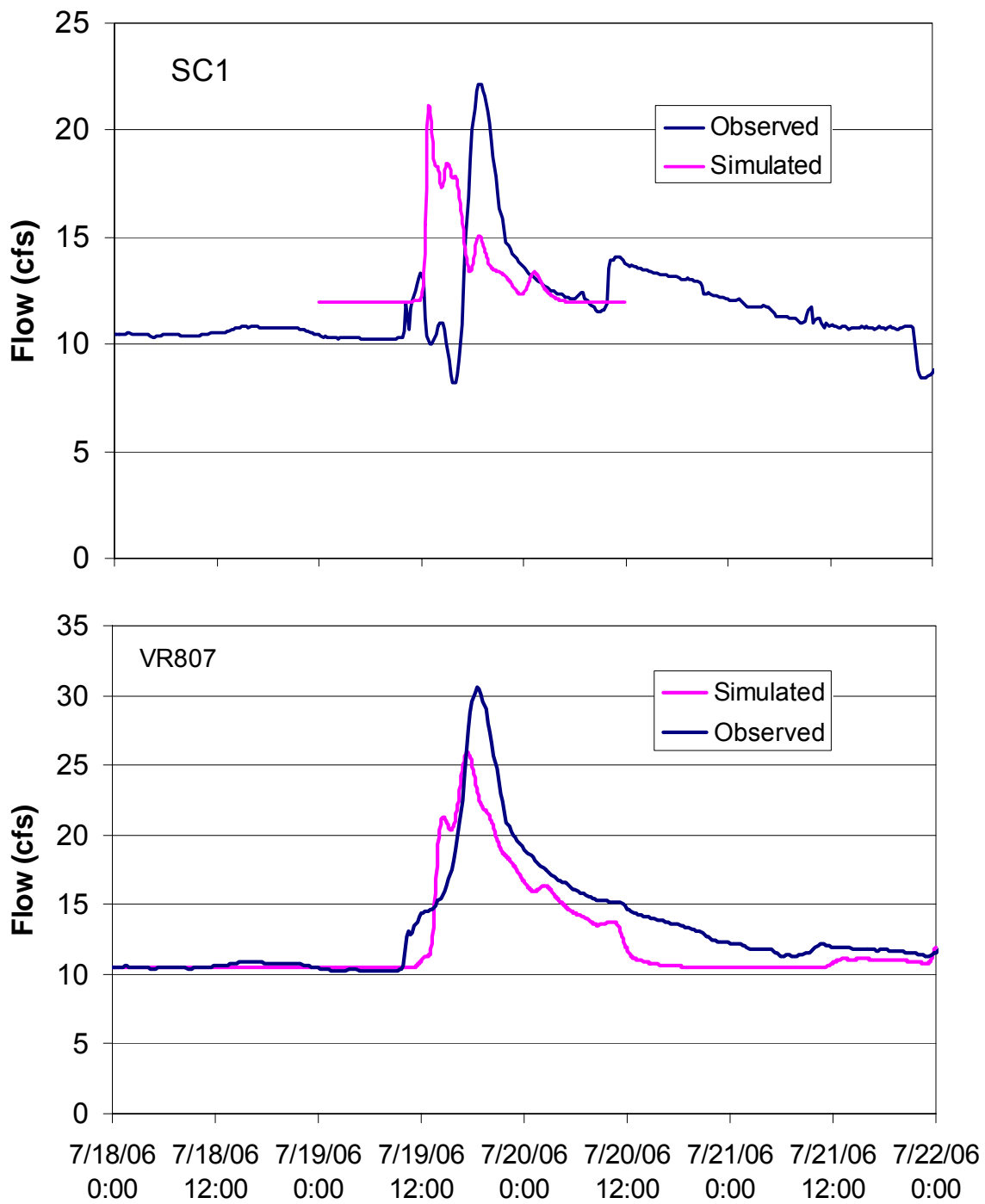


Figure 6.3. Measured and simulated stream flows during and after the July 19, 2006 rainfall event. Flow is measured at VR807 (Figure 6.1). The observed flow at SC1 (lower end of South Creek) was estimated by taking the difference between flow measurements at stations VR807 and SC804.

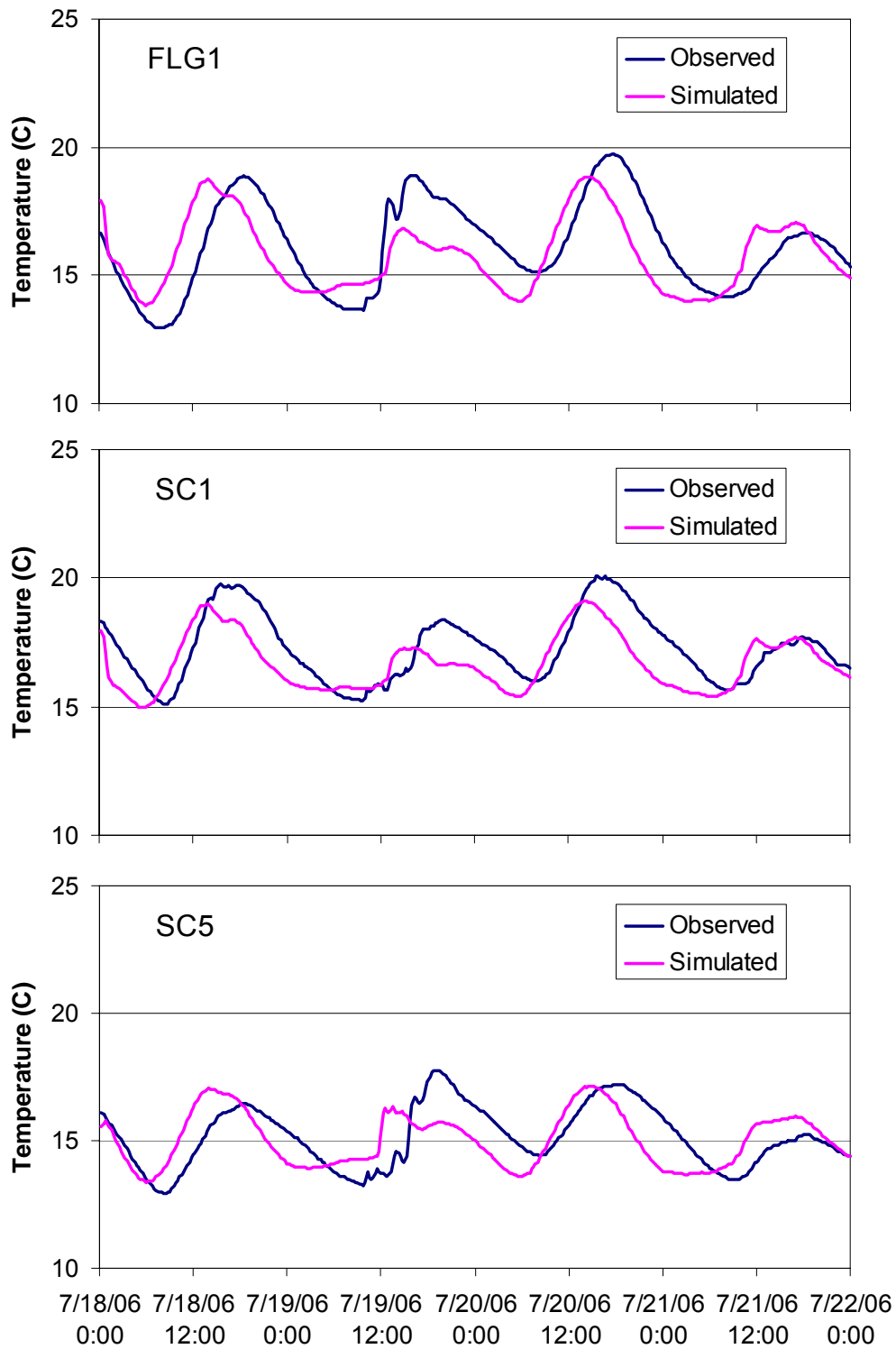


Figure 6.4. Simulated and observed stream temperature time series at three stations on South Creek, during the July 19, 2006 rainfall event. The locations of the three stations are shown in Figure 6.2.

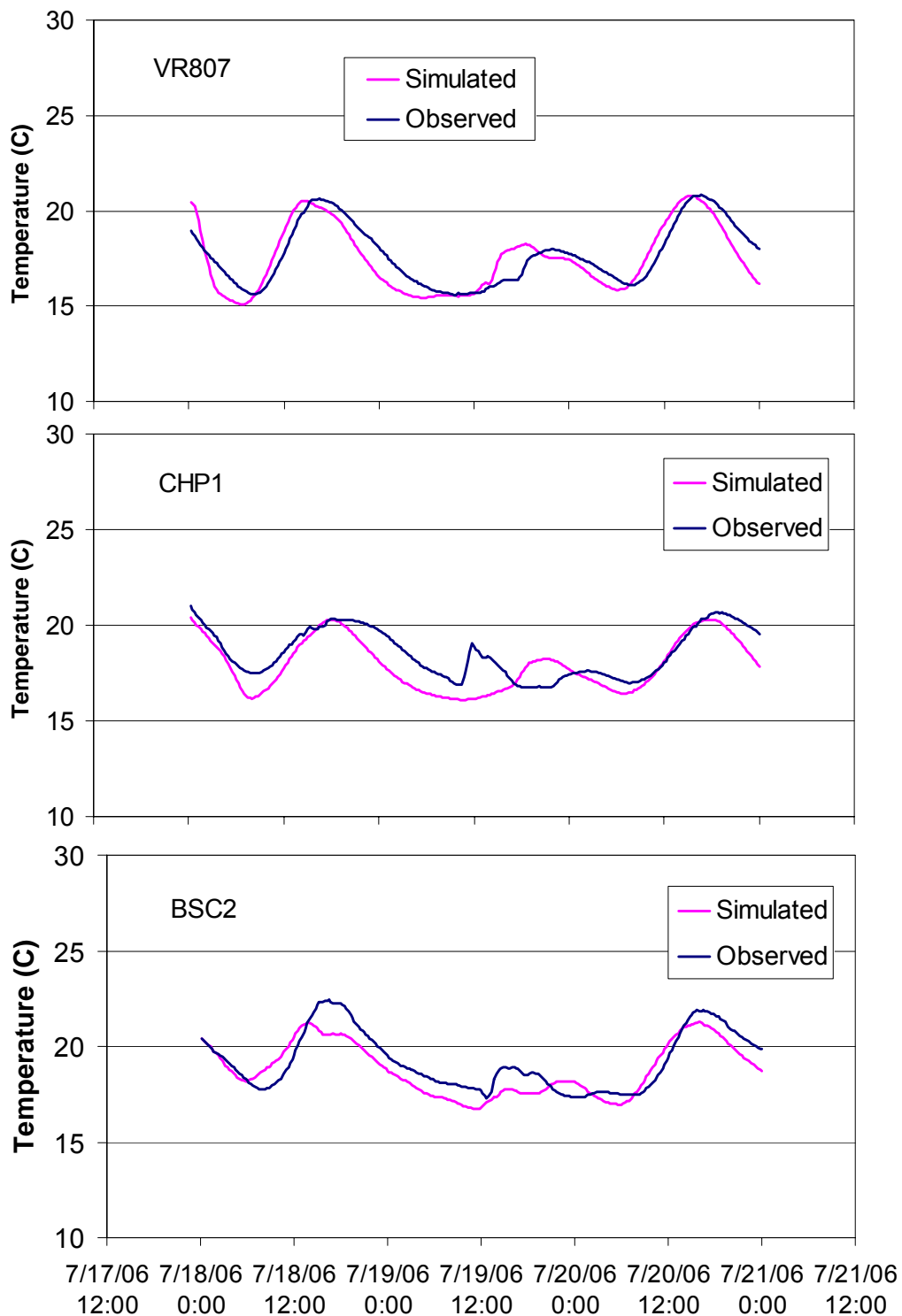


Figure 6.5. Simulated and observed stream temperature time series at three stations on the Vermillion River main stem, during the July 19, 2006 rainfall event. The locations of the three stations are shown in Figure 6.2.



## 7. The Combined Response of the Vermillion River to the Design Storm

This section summarizes the simulation results for the combined response of the Vermillion River to the ½" design storm (Appendix II), using surface runoff inputs from the 35 sub-watersheds (Figure 4.2), and using the baseflow scenario without the Empire WWTP effluent (Figure 3.1) as the initial condition. The stream flow and temperature simulation was performed for a period of 4 days, starting at midnight on the specified day of the design storm (July 25) and continuing for 3 days after the storm, to fully capture the response at the lower end of the main stem at Goodwin Avenue. The flow analysis was run at 1 to 5 minute time steps, with smaller tributaries with low baseflow conditions generally requiring a shorter time step to converge in the EPD-riv1 solver. The stream temperature analysis was performed at 5 minute time steps in all reaches. The climate conditions during, prior to, and after the design storm are described in Appendix II.

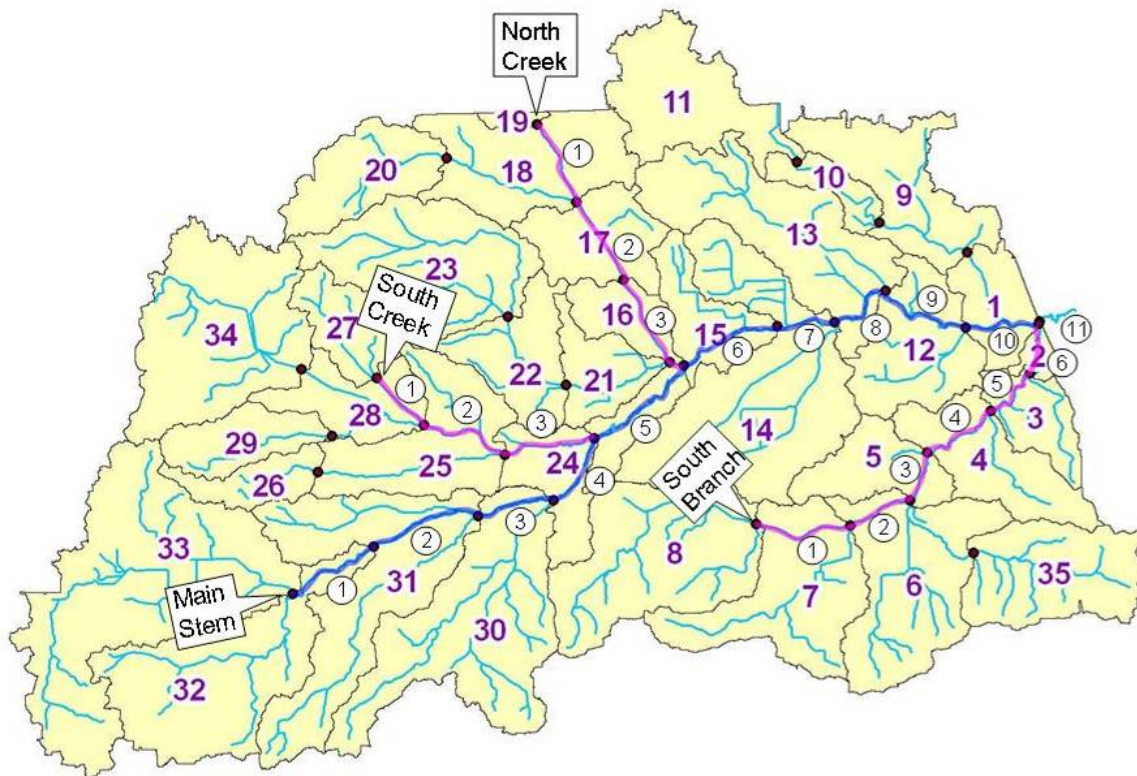


Figure 7.1. Reaches of the Vermillion River main stem (highlighted in blue) and major tributaries (highlighted in pink) for which results are given in this section. The circled numbers are the reach numbers referred to in Tables 7.1 and 7.2, while the uncircled numbers are the AES sub-watershed numbers.

The results given here focus on reach-averaged flow and temperature, with individual reaches defined between pairs of pour points. This was done for two reasons:

- 1) The individual pour points that supply surface runoff to the stream model do not, in all cases, represent actual point inflows of surface runoff. The inputs of surface runoff in the model may be more spatially concentrated than in the real system. The simulated surface runoff inputs will tend to create concentrated thermal hotspots, with relatively high local temperature changes.

Averaging flow and temperature changes over the reach between pour points may then give more realistic answers.

2) Reach-averaged changes may be more relevant to determining impacts on aquatic habitat, since localized warm spots can be avoided by fish.

The flow and temperature results were averaged over reaches between pairs of pour points, as listed in Tables 7.1 and 7.2, and illustrated in Figure 7.1. An example of simulated stream temperature at the spatial resolution of the model and for reach-averaged values is given in Figure 7.2. Simulated stream temperatures are plotted for cases with and without the surface runoff inputs, approximately 8 hours after the design storm event. The reach-averaging process maintains the overall spatial trends over scales of several miles, but smoothes the response from individual pour points.

The reach-averaged flow response to surface runoff from the design storm is illustrated in Figures 7.3 and 7.4, for the main stem, North Creek, South Creek, and South Branch. The increase in stream flow due to surface runoff ( $\Delta Q$ ) and the duration that  $\Delta Q$  exceeds 1 cfs are plotted for each reach. In general, the magnitude of  $\Delta Q$  increases with downstream distance, as the surface runoff inputs accumulate and add together, from 1 to 10 cfs increases at the upstream boundaries to a maximum of 47 cfs in the main stem, downstream of North Creek. At the lower end of the main stem, the maximum  $\Delta Q$  decreases slightly, due to broadening of the flow peak. The duration of the flow increase also increases with downstream distance, from 4 hours or less at the upstream ends of the main stem and tributaries to 40 hours at the downstream end of the main stem.

The stream temperature time series given in Figure 5.2 suggest that maximum stream temperatures during dry, warm and sunny days may match or exceed maximum stream temperatures due to surface runoff inputs from rainfall events. To examine this point further for the design storm conditions, the maximum stream temperature prior to the rainfall event (midnight – 4 pm, July 25) and after the rainfall event (4 pm July 25 – 12 am July 26) has been plotted in Figure 7.5 as a function of distance along the main stem. The corresponding channel shading coefficients and groundwater input rates used for the analysis are also given. For the main stem, maximum stream temperatures reached during the surface runoff are slightly lower than the temperatures prior to the design storm event. For the design storm, the maximum temperatures appear to be determined mainly by channel shading and groundwater inputs more than surface runoff inputs.

In addition, the maximum stream temperature change due to surface runoff input for the design storm has been plotted in Figure 7.5. These temperature differences were calculated by running the stream temperature model with and without the surface runoff inputs, e.g. as shown in Figure 5.2. Surface runoff from the design storm causes up to 2°C increase in stream temperature at the far upstream end of the main stem, where baseflow is small, and downstream of South Creek, where significant surface runoff from the South Creek watershed enters the main stem and flows into a relatively cool section of the main stem.

In addition to maximum stream temperatures, the duration of stream temperature exceedances is also important for the evaluation of aquatic habitat. In Figure 7.6 the simulated duration of the

stream temperature exceedance,  $T > 20\text{ }^{\circ}\text{C}$ , in the main stem, with and without surface runoff inputs from the design storm has been plotted. The temperature exceedance duration is calculated over the period 12 am to 12 pm July 25. The longest duration of the temperature exceedance is 15-17 hours and occurs at the upstream end of the main stem and upstream of the confluence with South Creek. The design storm runoff leads to only minor increases in the temperature exceedance duration, from an average of 7.9 hours to 8.7 hours.

Similar maximum stream temperature results for the major tributaries (North Creek, South Creek, South Branch) are given in Figures 7.7 and 7.8, and summarized in Table 7.2. In contrast to the main stem, the lower portions of both North Creek and South Creek show significantly higher maximum stream temperatures during the runoff event compared to dry weather conditions prior to the storm event, with peak temperatures in the range of 21 to 22  $^{\circ}\text{C}$ . Temperature exceedance duration plots for the tributaries are given in Figures 7.9 and 7.10. South Creek and North Creek both show significant increases (2-6 hours) in the duration of stream temperature exceeding 20 $^{\circ}\text{C}$  due to surface runoff.

Table 7.1. Reach-averaged flow and temperature statistics for the response of the Vermillion River main stem to the 1/2" design storm. The AES, Inc. inputs are numbered in Figure 7.1.

Reach	Upstream Node		Mean Temp ( $^{\circ}\text{C}$ )	Mean Baseflow (cfs)	Max Temp ( $^{\circ}\text{C}$ )		Max $\Delta\text{T}$ ( $^{\circ}\text{C}$ )	Max $\Delta\text{Q}$ (cfs)
	River Sta. (miles)	AES Input			Pre-storm	Runoff		
1	36.020	33	20.9	0.25	23.0	22.6	2.1	5.6
2	34.640	32	17.5	1.13	19.6	19.3	1.8	4.8
3	31.100	31	19.6	2.53	21.7	21.5	0.7	5.1
4	28.650	30	20.8	3.25	22.8	22.6	0.4	5.2
5	26.670	24	18.9	12.25	20.1	20.1	1.9	19.8
6	23.300	16	18.8	22.65	20.1	19.8	0.9	45.6
7	21.12	15	19.1	25.75	20.8	20.7	0.3	46.6
8	19.47	14	19.3	27.83	20.8	20.7	0.2	44.1
9	17.35	13	19.6	30.71	20.6	20.4	0.1	40.0
10	14.93	12	19.9	34.34	21.1	20.2	0.1	38.1
11	12.59	1	19.9	43.23	20.9	20.3	0.1	36.8

Reach	Upstream Node		Duration (hours)					
	River Sta. (miles)	AES Input	$T > 20^{\circ}\text{C}$ w/ SR	$T > 20^{\circ}\text{C}$ w/o SR	$\Delta\text{T} > 1^{\circ}\text{C}$	$\Delta\text{T} > 2^{\circ}\text{C}$	$\Delta\text{T} > 4^{\circ}\text{C}$	$\Delta\text{Q} > 1$ cfs
1	36.020	33	17.75	14.75	2.5	0.25	0	8.5
2	34.640	32	0	0	1.5	0	0	12.8
3	31.100	31	9	7.75	0	0	0	17.3
4	28.650	30	17.25	16.25	0	0	0	18.8
5	26.670	24	1.75	1.75	3	0	0	25.5
6	23.300	16	1.25	1.25	0	0	0	28.5
7	21.12	15	4.75	4.75	0	0	0	29.0
8	19.47	14	5.75	5.75	0	0	0	29.0
9	17.35	13	8.5	8	0	0	0	29.8
10	14.93	12	9.25	9	0	0	0	36.5
11	12.59	1	9.5	8.5	0	0	0	40.0

Table 7.2. Reach-averaged flow and temperature statistics for the response of the Vermillion River tributaries (South Creek, North Creek, South Branch) to the ½” design storm. The AES inputs are numbered in Figure 7.1.

Reach	Upstream Node		Mean Temp (C)	Mean Baseflow (cfs)	Max Temp (C)		Max ΔT (C)	Max ΔQ (cfs)
	River Sta. (miles)	AES Input			Pre-storm	Runoff		
South Creek								
1	5.642	27	17.6	1.0	19.6	19.1	0.5	8.5
2	3.219	28	18.3	3.5	19.4	21.8	3.5	17.8
3	1.443	25	17.6	6.9	18.2	21.0	3.7	25.1
North Creek								
1	4.795	19	20.3	0.5	23.1	22.5	1.2	1.4
2	3.619	18	19.1	2.7	20.3	21.5	3.7	21.1
3	2.038	17	18.3	5.4	19.6	20.2	3.3	21.8
South Branch								
1	9.106	8	17.1	1.1	18.7	18.4	1.7	0.8
2	7.294	7	17.4	2.2	19.2	19.0	1.0	2.2
3	5.714	6	18.0	3.9	20.2	19.6	0.8	5.1
4	4.443	5	18.2	4.7	20.2	20.2	0.6	4.6
5	2.737	4	18.1	5.6	19.2	19.8	0.7	4.7
6	1.312	3	18.1	6.4	18.9	19.2	0.6	4.7

Reach	Upstream Node		Duration (hours)					
	River Sta. (miles)	AES Input	T>20 °C w/ SR	T > 20 °C w/o SR	ΔT>1 °C	ΔT>2 °C	ΔT>4 °C	ΔQ>1 cfs
South Creek								
1	5.642	27	0	0	0	0	0	3.5
2	3.219	28	3.25	0	7.25	3	0	15
3	1.443	25	2.75	0	6	4	0	15
North Creek								
1	4.795	19	12.25	9	4.5	0	0	2.75
2	3.619	18	7.25	2	5.5	4.25	0	9
3	2.038	17	1.5	0	3	2.25	0	9.25
South Branch								
1	9.106	8	0	0	3.75	0	0	0
2	7.294	7	0	0	1	0	0	2.5
3	5.714	6	1	1	0	0	0	4.5
4	4.443	5	2.25	2.25	0	0	0	5
5	2.737	4	0	0	0	0	0	7.5
6	1.312	3	0	0	0	0	0	9.5

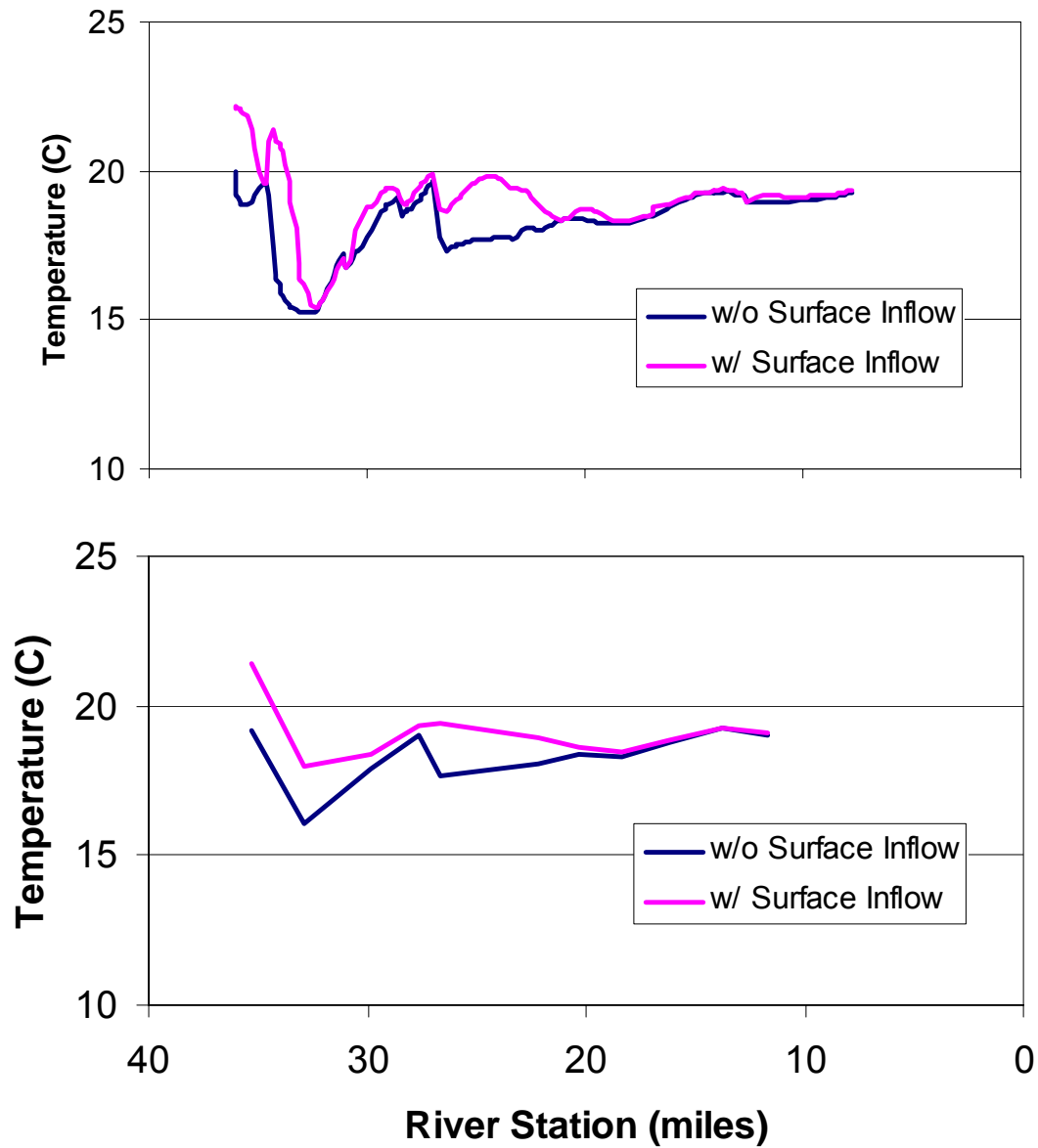


Figure 7.2. Simulated stream temperature versus distance with and without surface inflows from the design storm. Values are for a time 8 hours after the onset of rainfall (midnight, July 25), for 184 model nodes (upper panel) and for 14 reach-averaged values (lower panel).

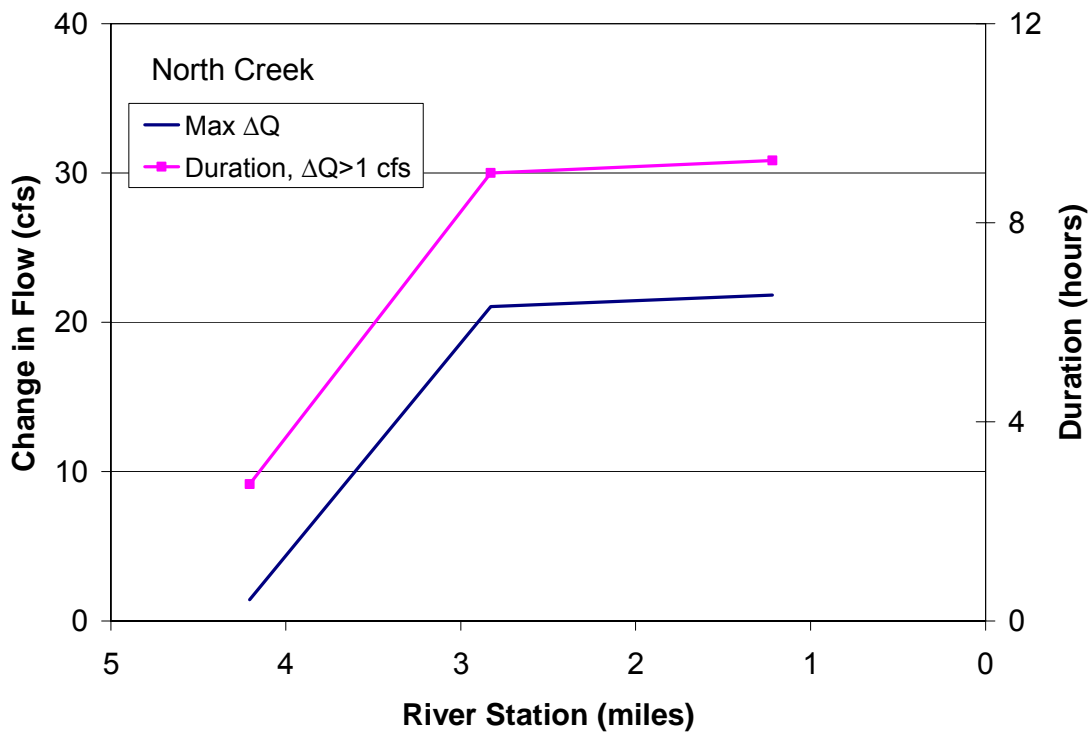
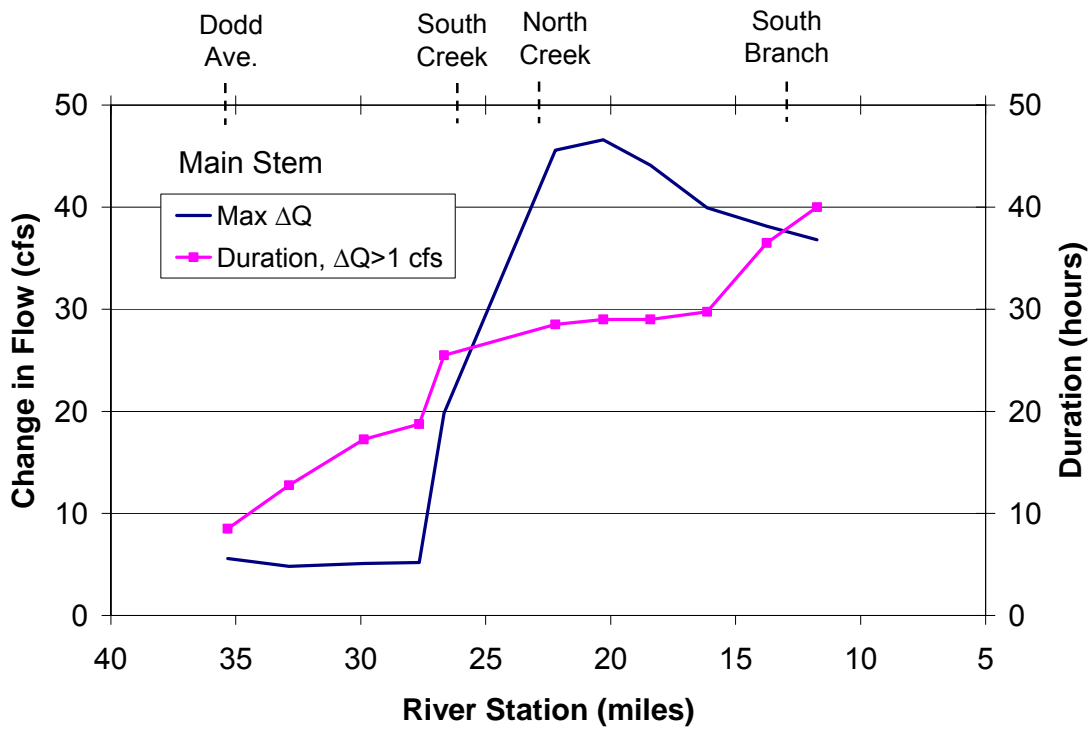


Figure 7.3. Maximum change in flow due to runoff ( $\Delta Q$ ), and duration of increased flow ( $\Delta Q > 1$  cfs) for the main stem (upper panel) and North Creek (lower panel) in response to the design storm. Reach-averaged values are plotted over distance.

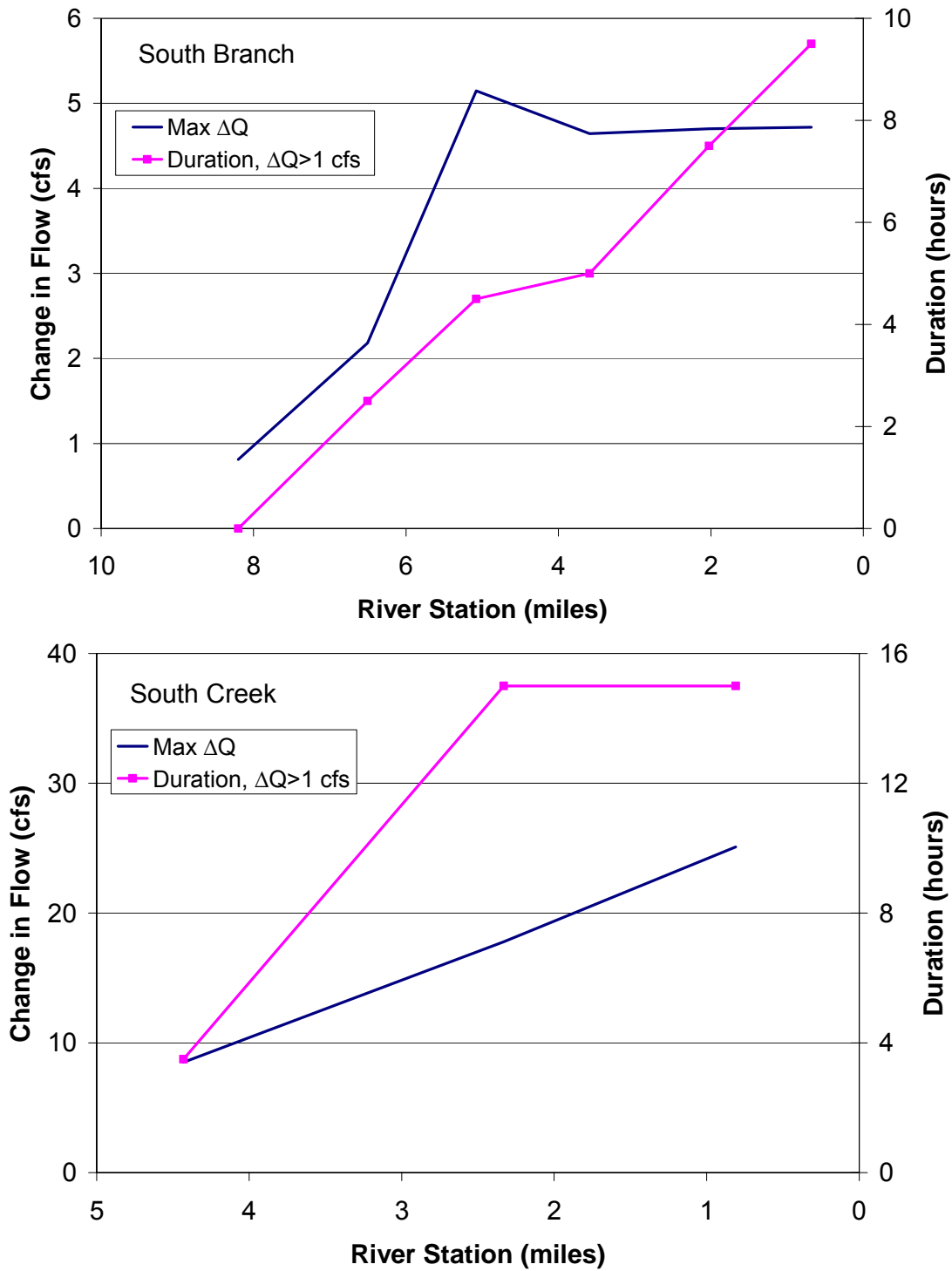


Figure 7.4. Maximum change in flow due to runoff ( $\Delta Q$ ) and duration of increased flow ( $\Delta Q > 1$  cfs) for the South Branch (upper panel) and South Creek (lower panel) in response to the design storm. Reach-averaged values are plotted over distance.

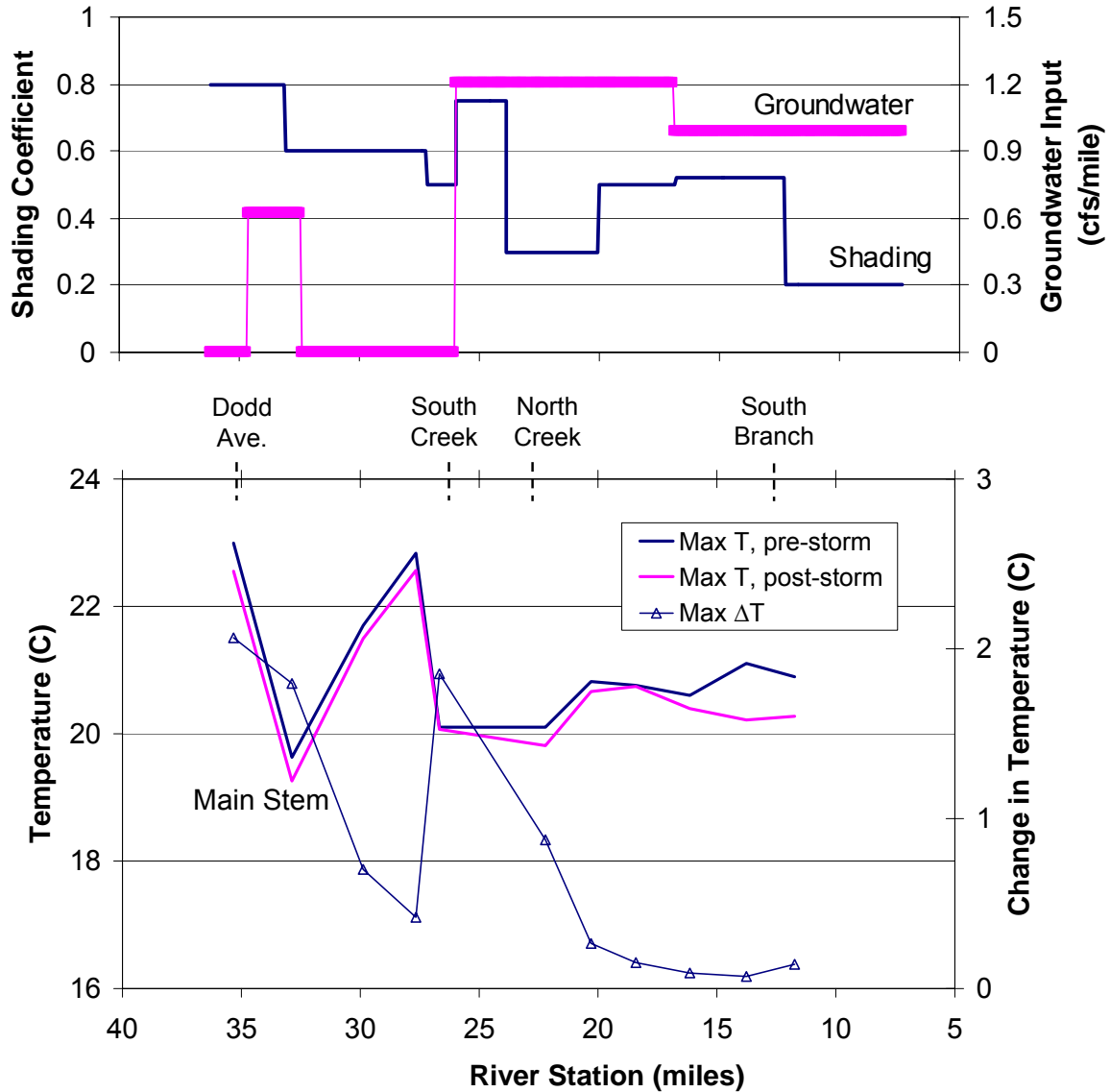


Figure 7.5. Calibrated channel shading coefficient and groundwater input rate along the main stem (upper panel). Maximum stream temperature (Max T) before and after storm event and maximum change in stream temperature due to runoff ( $\Delta T$ ) for the main stem in response to the design storm (lower panel).



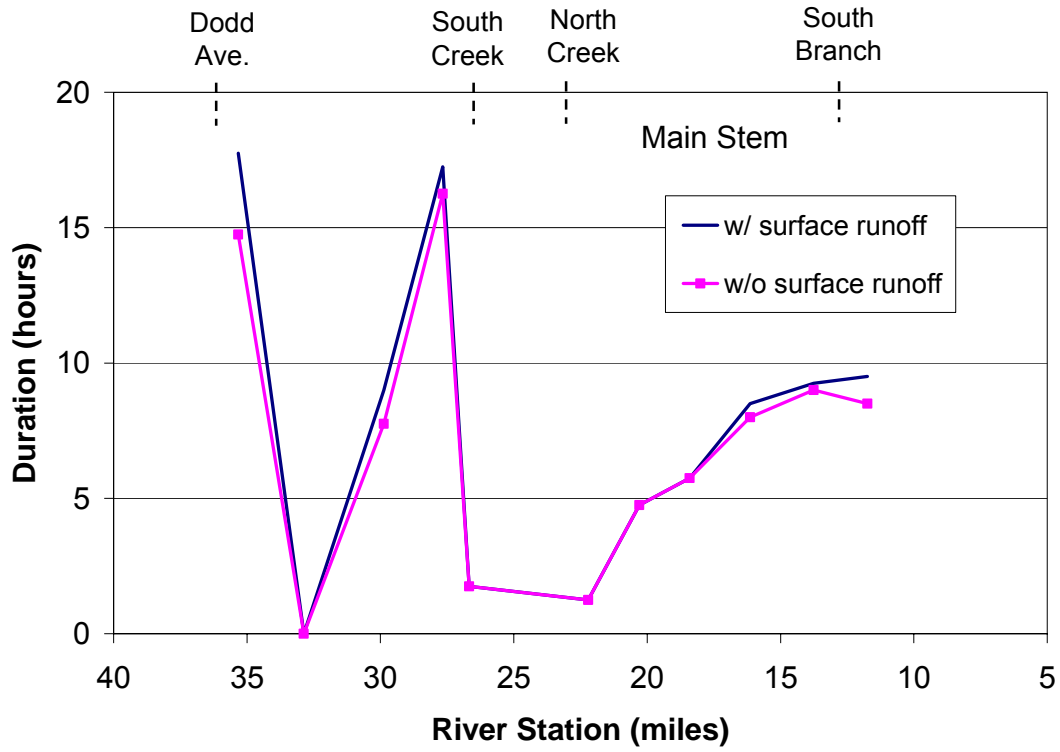


Figure 7.6. Duration of temperature exceedance ( $T > 20^{\circ}\text{C}$ ) in the main stem in response to the design storm. Reach-averaged values are plotted over distance.

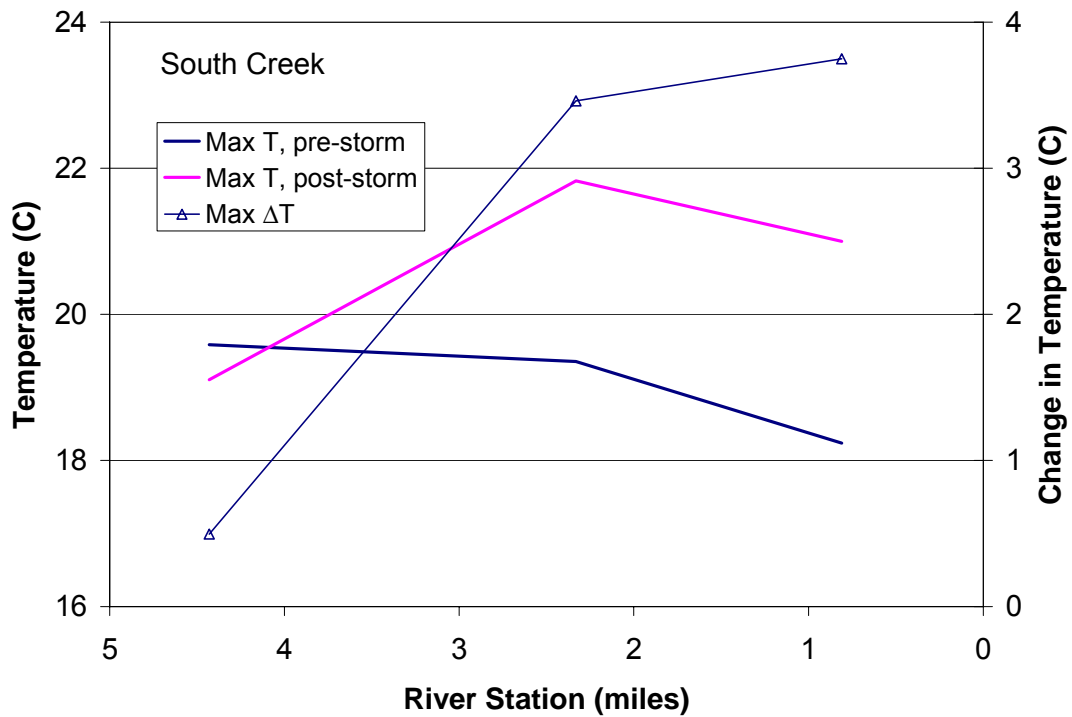
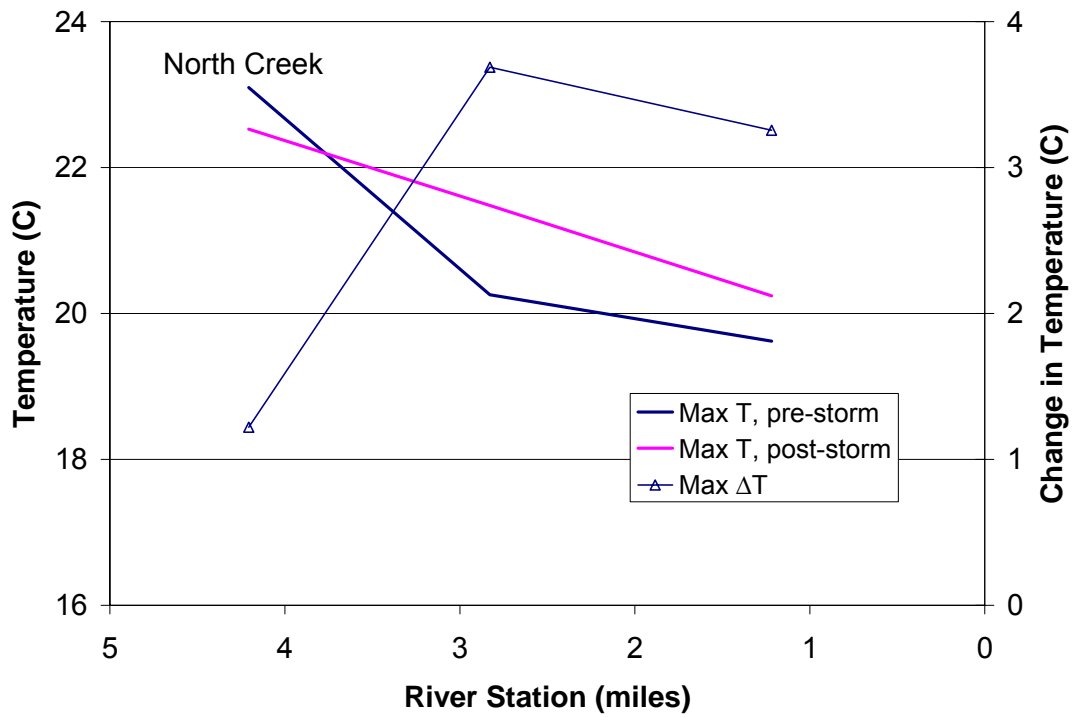


Figure 7.7. Maximum stream temperature (Max T) before and after storm event and maximum change in stream temperature due to runoff ( $\Delta T$ ) for North Creek (upper panel) and South Creek (lower panel) in response to the design storm.

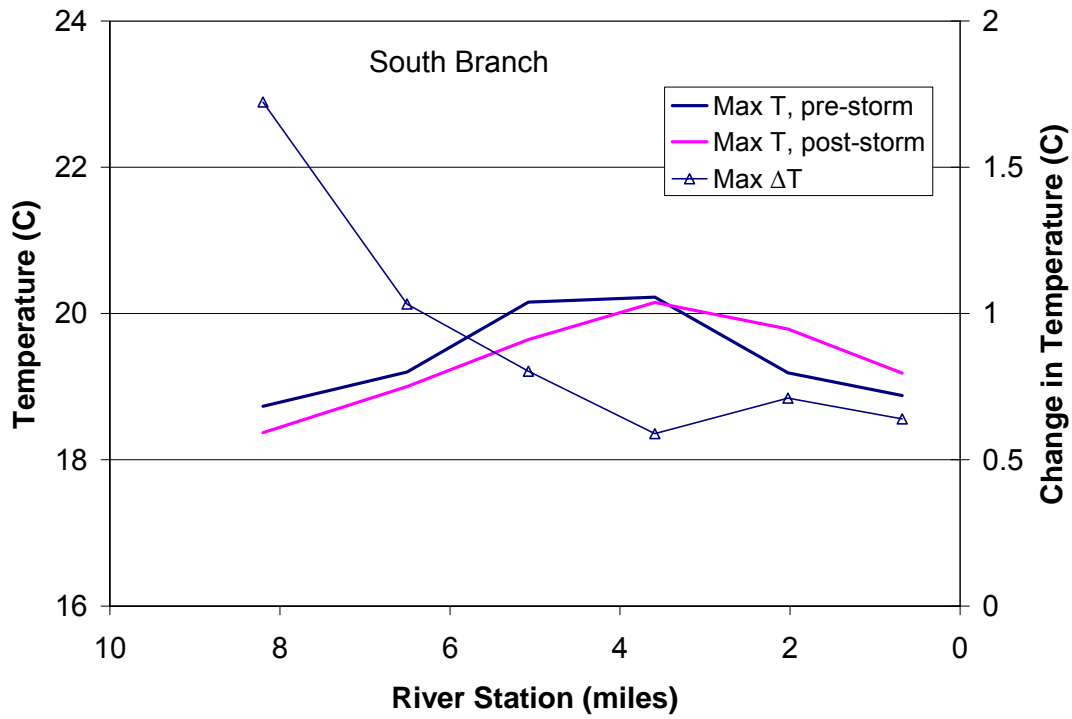


Figure 7.8. Maximum stream temperature (Max T) before and after storm event and maximum change in stream temperature due to runoff ( $\Delta T$ ) in South Branch in response to the design storm.

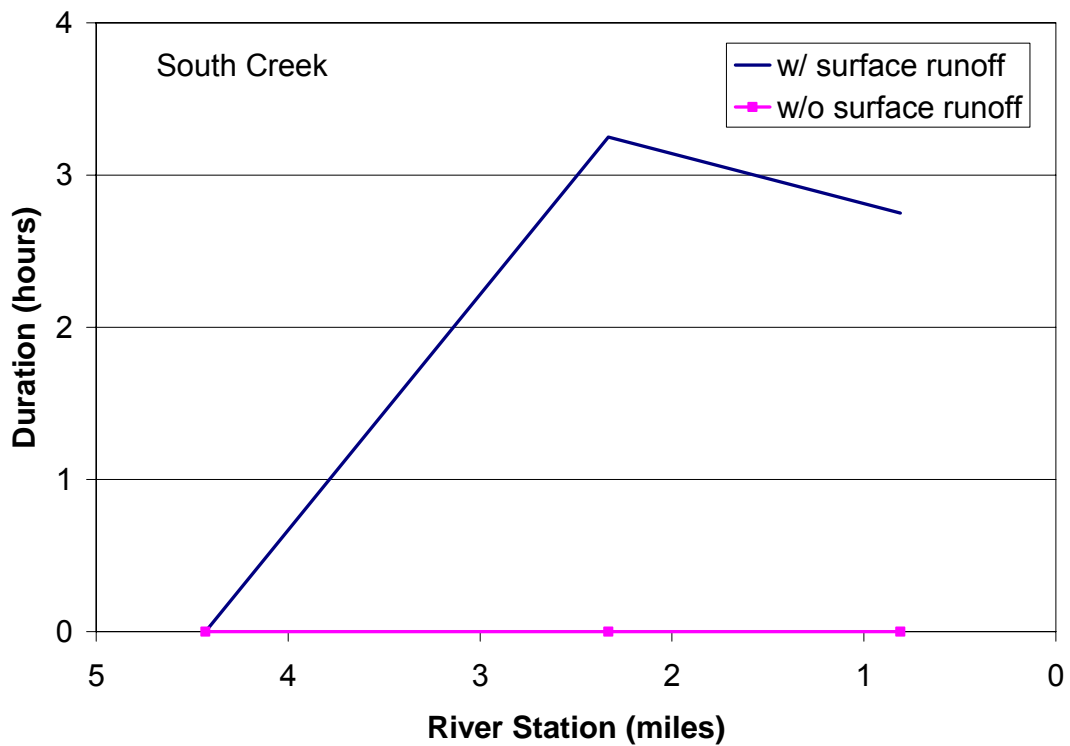
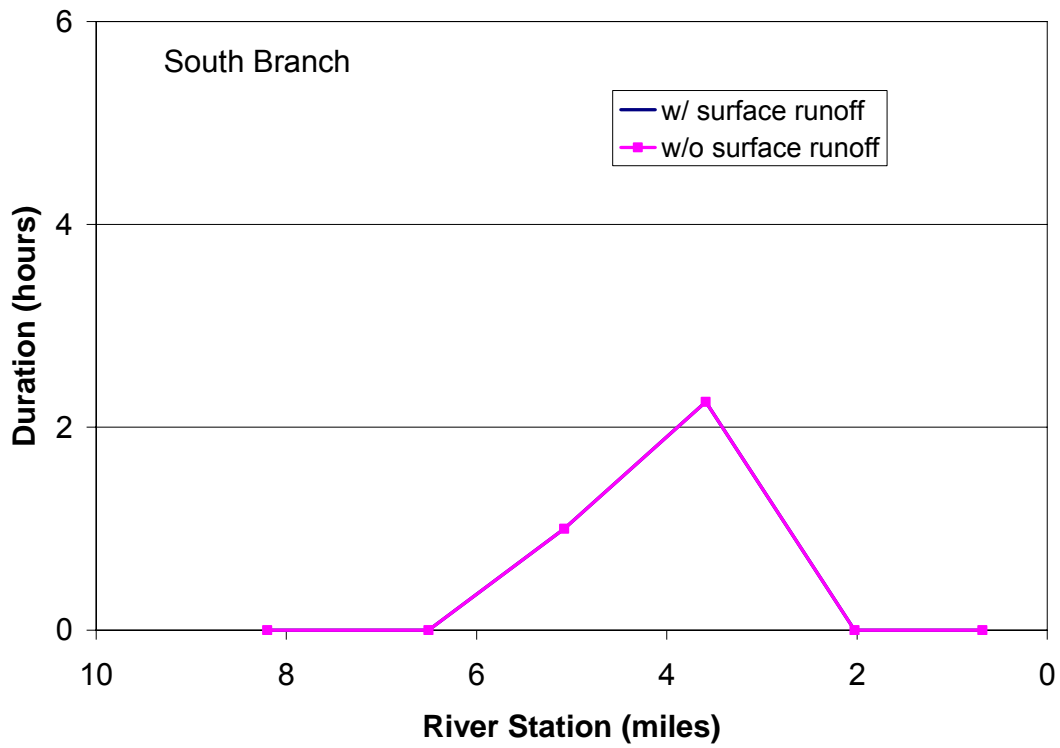


Figure 7.9. Duration of temperature exceedance ( $T > 20^{\circ}\text{C}$ ) in South Branch (upper panel) and South Creek (lower panel) in response to the design storm.

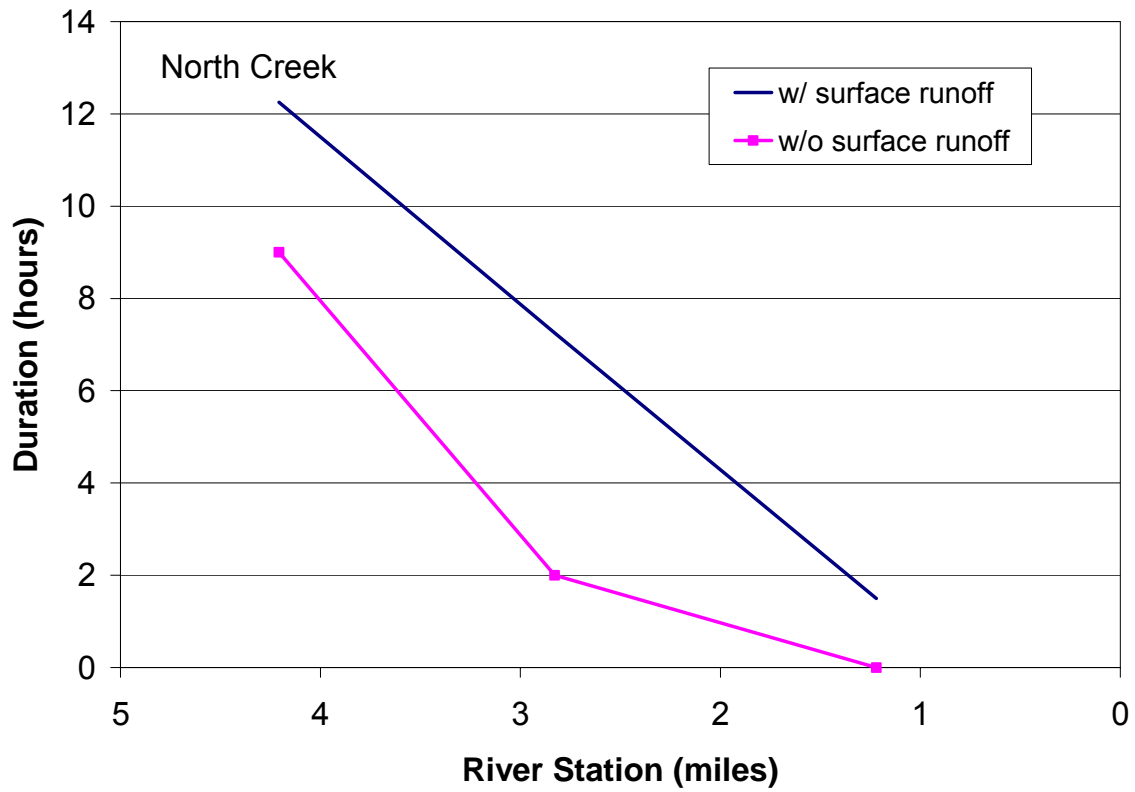


Figure 7.10. Duration of temperature changes ( $\Delta T = 1, 2$  and  $4^{\circ}\text{C}$ ) in South Branch (upper panel) and South Creek (lower panel) in response to the design storm. Reach-averaged values are plotted over distance.

## **8. Effects of Land Development and Mitigation Scenarios**

Using the stream thermal impact model several future urban development scenarios and several thermal mitigation scenarios in the Vermillion River watershed were studied in support of the EPA-funded thermal trading study. The mitigation study was performed on a portion of the Vermillion River watershed shown in Figure 8.1 and including most of South Creek and a portion of the main stem from South Creek to the Empire WWTP. The ½” design storm (Appendix II) was used as the basis for all analyses.

### **Development Scenarios**

Three future development scenarios were examined for sub-watersheds in South Creek; development scenarios were created in sub-watersheds 26-29 (Figure 8.1):

- 1) 200-acre mixed-use development in sub-watershed 26.
- 2) 50% development in sub-watersheds 26-29.
- 3) 100% development in sub-watersheds 26-29.

In each case, distributions of pervious and impervious surfaces typical for present developments were used to modify the 10x10 m land use pixels in the land cover heat contribution model. This work was performed by AES. The land cover heat contribution model was then run for the three development cases, creating new surface runoff volumes and temperatures at the pour points for sub-watersheds 26-29.

### **Mitigation Scenarios**

Several mitigation scenarios were created in subwatersheds 15-16 and 24-25, to examine if upstream thermal impacts could be compensated for by downstream mitigation measures such as:

- a) restoration of farmed hydric soils to wetlands,
- b) addition of channel shading to unshaded stream reaches, and
- c) disconnection of commercial rooftop areas from surface runoff.

In total, nine cases with different combinations of development and mitigation were simulated. Eight cases (Case 1- Case 8) are listed below.

Case 1: present land use

Case 2: 50% development, no mitigation

Case 3: 100% development, no mitigation

Case 4: present land use, commercial roof disconnect

Case 5: 100% development, commercial roof disconnect

Case 6: present land use, added shading/sheltering

Case 7: 100% development, added shading/sheltering

Case 8: 100% Development, Added Shading and Commercial Roof Disconnect

The ninth case is the 200 acre development, which was analyzed separately. Mitigation scenario a) was found to have no influence on runoff and stream temperatures, because for both land uses (agriculture, wetland), there was no runoff volume for the ½” design storm.

The additional shading specified for the stream reaches is illustrated in Figure 8.2. The shading levels were increased to a reasonable maximum, based on calibrated shading coefficients for various sections of the river system. The highest attainable shading level decreases downstream as the channel widens.

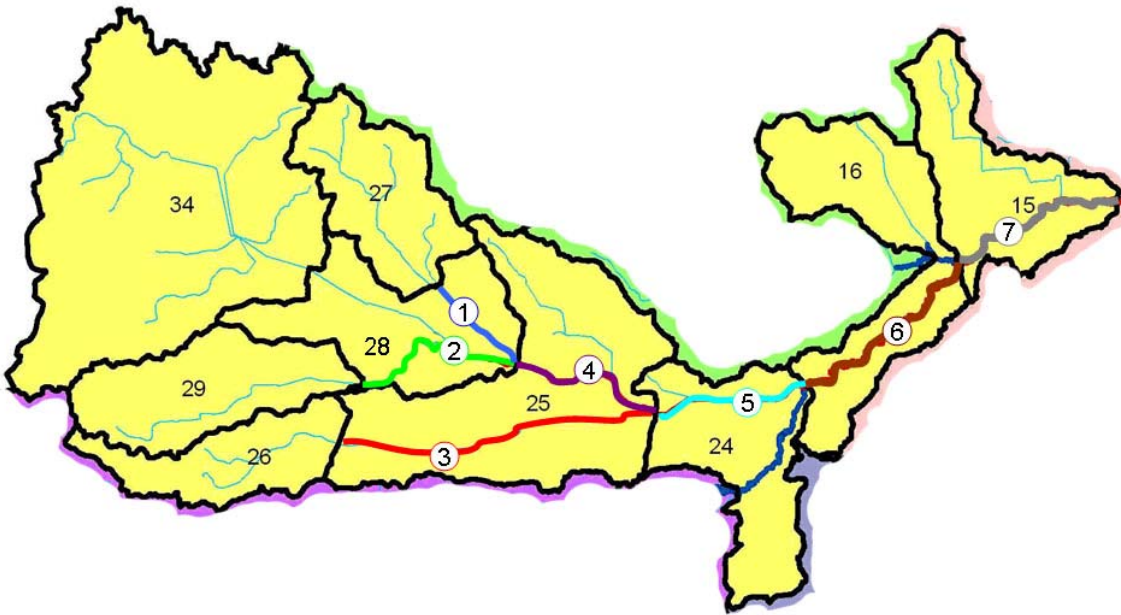


Figure 8.1. Reach numbers (circled) and sub-watershed numbers (not circled) in trading zone 1. In the trading scenario, development is added to sub-watersheds 26-29, while mitigation is added to sub-watersheds 15, 16, 24, and 25.

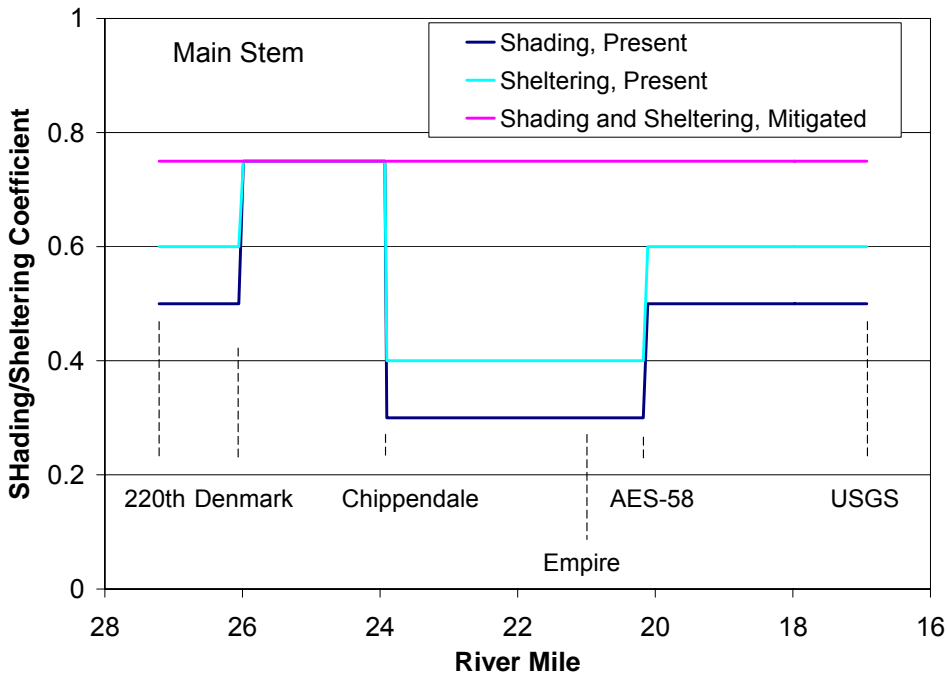
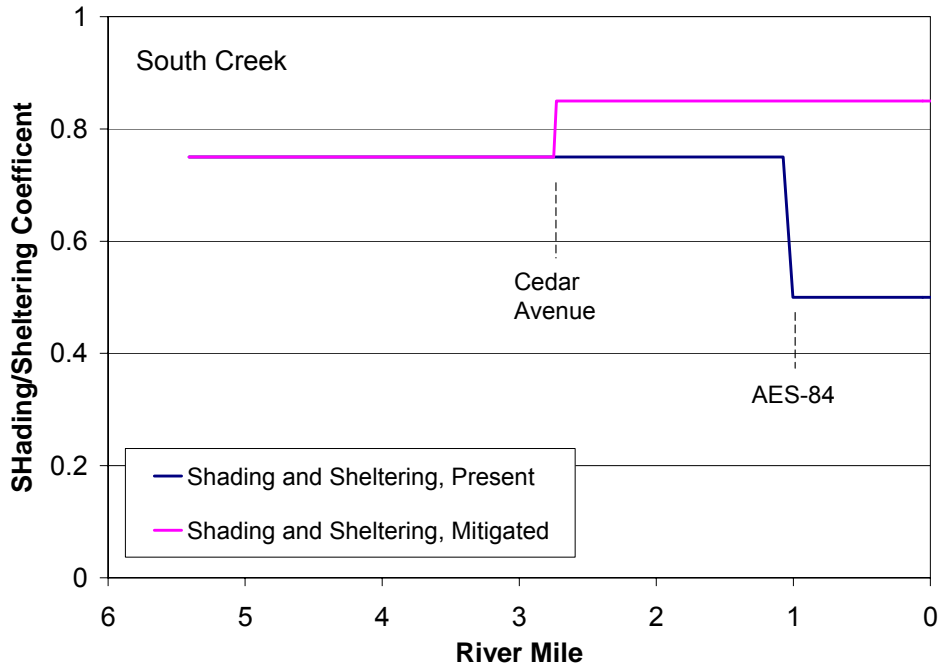


Figure 8.2. Increase in shading and wind sheltering in South Creek (upper panel) and the main stem of the Vermillion River (lower panel) for the mitigation scenarios. 0=no shading/sheltering, 1=complete shading/sheltering of the stream surface.



## Results: Impact of 200 Acre Mixed-use Development

The 200 acre mixed-use development case was simulated specifically to determine if the stream thermal impact model is capable of resolving the thermal impact of a single development. The development was inserted in the land cover heat contribution model in sub-watershed 26, with the simulated runoff entering the stream temperature model at the upstream end of Reach 3 (Figure 8.1). The addition of the 200 acre development increased the maximum stream temperature in Reach 3 noticeably, i.e. on the order of 2 °C for much of the reach (Figure 8.3). The change in stream temperature downstream of Reach 3 was minimal, i.e. on the order of 0.2 °C or less.

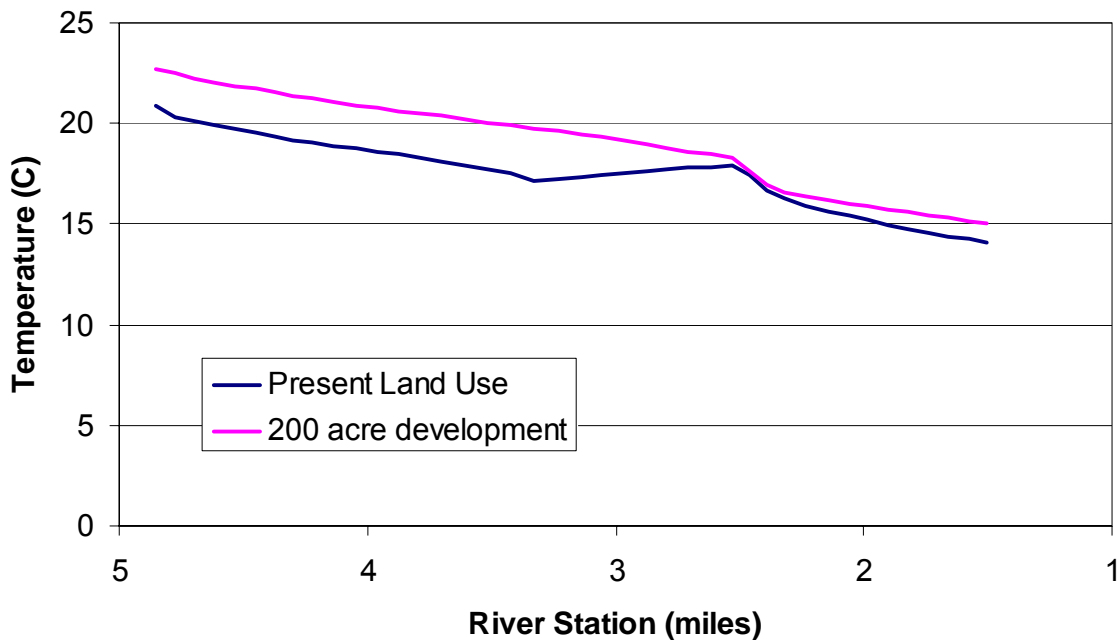


Figure 8.3. Simulated maximum stream temperature during runoff for present land use and for the addition of a 200 acre development, in response to the ½” design storm.

## Results: Land Development and Mitigation Cases 1 – 8

As with the design storm results given in Section 7, the results of the flow and temperature simulations are given as reach-averaged values, where each reach extends between two pour points. The reaches in South Creek and the main stem of the Vermillion used in this section are illustrated in Figure 8.1. The simulation results for cases 1 – 8 were analyzed as follows:

- 1) From the raw stream temperature simulation results for each case, the highest stream temperature during the runoff event was found for each point in each reach. The temperature maxima do not necessarily occur at the same time. Temperature maxima occurring during dry weather periods prior to runoff were ignored.

- 2) Within each of the seven reaches, the temperature maxima were processed to find the highest, lowest, and reach-averaged values. The location of the highest maximum temperature in each reach was also stored.
- 3) The total length of periods when simulated stream temperatures were above 20°C or above 23°C (temperature exceedance durations) during the runoff event was found for each point in each reach.
- 4) Within each of the seven reaches, the temperature exceedance durations were processed to find the highest, lowest, and reach-averaged values.

Although local temperature maxima and minima were calculated for each reach, the reach-averaged temperatures and durations may be the most relevant, as explained in Section 7. Tables 8.1 through 8.3 summarize the results for the eight cases in the seven stream reaches. Table 8.1 gives the simulation results for the nominal (present) case, and the 50% and 100% development cases with no mitigation. Table 8.2 gives the simulation results for the 5 cases with downstream mitigation. Results in Table 8.2 are given only for reaches 4 – 7, since the mitigation strategies were not applied to the upstream sub-watersheds (1-3). Table 8.3 gives the incremental differential changes in stream temperature parameters due to the various development and mitigation scenarios. The results are interpreted as follows:

Effects of development: The stream temperature increases due to the 50% and 100% development scenarios produce increases in the maximum stream temperatures during runoff ranging from 3 to 4°C in Reach 3 to values less than 0.1°C in the main stem near Empire. Reach 3 experiences the most temperature change due to development because it has a relatively low baseflow temperature (12 to 16°C) compared to other reaches. Reach 7 experiences the least temperature impact because 1) baseflow is higher, 2) higher temperature water inputs cool off over distance (Section 6), and 3) the unimpacted stream temperature is higher for the larger, wider stream channel. The 50% and 100% development cases also produce significant increases in the temperature exceedance durations ( $T > 20^\circ\text{C}$ ) of up to 2.5 hours. Exceedance durations also decrease slightly in the lower reaches in some cases. This is due to increased streamflow from upstream development leading to reduced impacts from downstream surface runoff inputs.

Effects of mitigation measures: The downstream mitigation scenarios produced relatively little thermal compensation for the adverse upstream development effects. While disconnecting commercial roof areas (Case 5) reduces the volume of high temperature runoff, relatively little commercial roof area was available in the downstream sub-watersheds (15, 16, 24, 25). As a result, downstream temperatures were only reduced by 0 – 0.25°C. Adding shading to the stream channels did not reduce stream temperature maxima during runoff, largely because atmospheric heat transfer, in many cases, acts to cool, rather than warm, stream temperatures during runoff events with warm inflows. There was somewhat more temperature reduction in Reach 7 (0.4°C), where the relatively large increase in shading (Figure 8.2) led to a lower stream temperature prior to the storm. In all reaches, increased shading did reduce stream temperature maxima on sunny days prior to and after the runoff event (Figure 8.4).

Table 8.1. Maximum stream temperatures and temperature exceedance durations above 20°C and 23°C for present and developed watershed cases with no mitigation. The maximum and minimum value within the reach and the reach-averaged value are given for each reach (Figure 1).

**Case 1: Present land use**

Reach	Max Temperature (°C)			Duration > 20°C (hours)			Duration > 23°C (hours)		
	High	Low	Average	High	Low	Average	High	Low	Average
1	24.28	20.93	23.12	3.67	2.33	3.27	2.50	0.00	0.57
2	24.32	20.47	22.71	6.08	2.08	4.48	2.50	0.00	0.44
3	20.84	14.10	17.62	0.75	0.00	0.03	0.00	0.00	0.00
4	23.52	21.72	23.47	4.67	2.33	3.81	0.75	0.00	0.18
5	21.86	20.65	22.18	3.00	2.33	2.83	0.00	0.00	0.00
6	20.75	19.41	20.46	6.42	0.00	1.19	0.00	0.00	0.00
7	20.55	19.46	20.62	3.17	0.00	1.04	0.00	0.00	0.00

**Case 2: 50% development, no mitigation**

1	24.24	21.99	23.54	3.83	3.25	3.74	2.50	0.00	0.80
2	24.19	21.47	23.31	7.33	5.00	6.21	3.00	0.00	0.82
3	22.26	16.00	20.09	2.08	0.00	1.12	0.00	0.00	0.00
4	23.64	22.10	23.77	6.67	5.50	6.06	1.00	0.00	0.31
5	22.14	21.21	22.71	5.08	1.75	2.38	0.00	0.00	0.00
6	21.21	19.90	20.93	5.83	0.00	1.44	0.00	0.00	0.00
7	20.55	19.72	20.66	3.17	0.00	1.03	0.00	0.00	0.00

**Case 3: 100% development, no mitigation**

1	24.19	22.41	23.70	4.00	3.25	3.97	3.00	0.00	0.99
2	24.14	22.16	23.70	7.83	5.42	6.82	3.25	0.00	1.02
3	22.89	18.26	21.39	3.50	0.00	2.43	0.00	0.00	0.00
4	24.00	22.12	23.83	7.83	5.58	6.32	0.75	0.00	0.24
5	22.14	21.23	22.74	5.83	1.50	3.76	0.00	0.00	0.00
6	21.23	19.98	20.94	6.83	0.00	1.43	0.00	0.00	0.00
7	20.55	19.80	20.69	3.17	0.00	1.03	0.00	0.00	0.00

Table 8.2. Maximum stream temperatures and temperature exceedance durations above 20°C and 23°C for present and developed watershed cases with mitigation. The maximum and minimum value within the reach and the reach-averaged value are given for each reach (Figure 1).

<b>Case 4: Present land use, commercial roof disconnect</b>									
Reach	Max Temperature (°C)			Duration > 20°C (hours)			Duration > 23 °C (hours)		
	High	Low	Average	High	Low	Average	High	Low	Average
4	23.52	21.72	23.47	4.67	2.33	3.81	0.75	0.00	0.18
5	21.57	20.40	21.91	2.92	1.75	2.59	0.00	0.00	0.00
6	20.63	19.29	20.23	6.08	0.00	0.77	0.00	0.00	0.00
7	20.55	19.46	20.61	3.17	0.00	1.04	0.00	0.00	0.00
<b>Case 5: 100% development, commercial roof disconnect</b>									
4	24.00	22.12	23.83	7.83	5.58	6.32	0.75	0.00	0.24
5	22.03	20.99	22.52	5.75	1.25	3.48	0.00	0.00	0.00
6	20.99	19.77	20.70	6.33	0.00	1.00	0.00	0.00	0.00
7	20.55	19.71	20.65	3.17	0.00	1.03	0.00	0.00	0.00
<b>Case 6: Present land use, added shading/sheltering</b>									
4	23.52	21.71	23.47	4.67	2.33	3.81	0.75	0.00	0.18
5	21.83	20.66	22.18	3.00	2.33	2.82	0.00	0.00	0.00
6	20.75	19.41	20.46	6.42	0.00	1.19	0.00	0.00	0.00
7	20.55	19.46	20.62	3.17	0.00	1.04	0.00	0.00	0.00
<b>Case 7: 100% development, added shading/sheltering</b>									
4	24.00	22.11	23.83	7.83	5.58	6.32	0.75	0.00	0.24
5	22.14	21.23	22.73	5.75	1.92	3.85	0.00	0.00	0.00
6	21.23	19.97	20.93	3.25	0.00	1.32	0.00	0.00	0.00
7	19.95	19.42	20.29	0.00	0.00	0.00	0.00	0.00	0.00
<b>Case 8: 100% development, added shading and commercial roof disconnect</b>									
4	24.00	22.12	23.83	7.83	5.58	6.32	0.75	0.00	0.24
5	22.03	20.98	22.51	5.75	1.25	3.53	0.00	0.00	0.00
6	20.98	19.76	20.69	2.75	0.00	0.89	0.00	0.00	0.00
7	19.79	19.28	20.14	0.00	0.00	0.00	0.00	0.00	0.00

Table 8.3. Change in maximum temperature and durations values due to development and mitigation. Maximum stream temperatures and temperature exceedance durations above 20°C and 23°C for present and developed watershed cases with mitigation. The maximum and minimum value within the reach and the reach-averaged value are given for each reach (Figure 1).

<b>Effect of 50% development (Case 2 - Case 1)</b>						
Reach	Change in Max Temperature (°C)		Change in Duration T > 20°C (hours)		Change in Duration T > 23°C (hours)	
	High	Average	High	Average	High	Average
1	-0.04	0.42	0.17	0.48	0.00	0.22
2	-0.13	0.60	1.25	1.73	0.50	0.38
3	1.42	2.47	1.33	1.09	0.00	0.00
4	0.12	0.29	2.00	2.26	0.25	0.13
5	0.28	0.53	2.08	-0.45	0.00	0.00
6	0.46	0.47	-0.58	0.25	0.00	0.00
7	0.00	0.04	0.00	-0.01	0.00	0.00
<b>Effect of 100% development (Case 3 - Case 1)</b>						
1	-0.09	0.58	0.33	0.70	0.50	0.42
2	-0.18	0.99	1.75	2.34	0.75	0.59
3	2.05	3.77	2.75	2.40	0.00	0.00
4	0.48	0.36	3.17	2.51	0.00	0.06
5	0.28	0.56	2.83	0.93	0.00	0.00
6	0.48	0.48	0.42	0.23	0.00	0.00
7	0.00	0.07	0.00	-0.01	0.00	0.00
<b>Effect of commercial roof disconnect (Case 5 - Case 3)</b>						
4	0.00	0.00	0.00	0.00	0.00	0.00
5	-0.11	-0.22	-0.08	-0.29	0.00	0.00
6	-0.24	-0.24	-0.50	-0.42	0.00	0.00
7	0.00	-0.04	0.00	0.00	0.00	0.00
<b>Effect of added shading/sheltering (Case 7 - Case 3)</b>						
4	0.00	0.00	0.00	0.00	0.00	0.00
5	0.00	0.00	-0.08	0.08	0.00	0.00
6	0.00	-0.01	-3.58	-0.10	0.00	0.00
7	-0.60	-0.40	-3.17	-1.03	0.00	0.00
<b>Effect of commercial roof disconnect and added shading (Case 8 - Case 3)</b>						
4	0.00	0.00	0.00	0.00	0.00	0.00
5	-0.11	-0.22	-0.08	-0.23	0.00	0.00
6	-0.25	-0.25	-4.08	-0.53	0.00	0.00
7	-0.76	-0.55	-3.17	-1.03	0.00	0.00

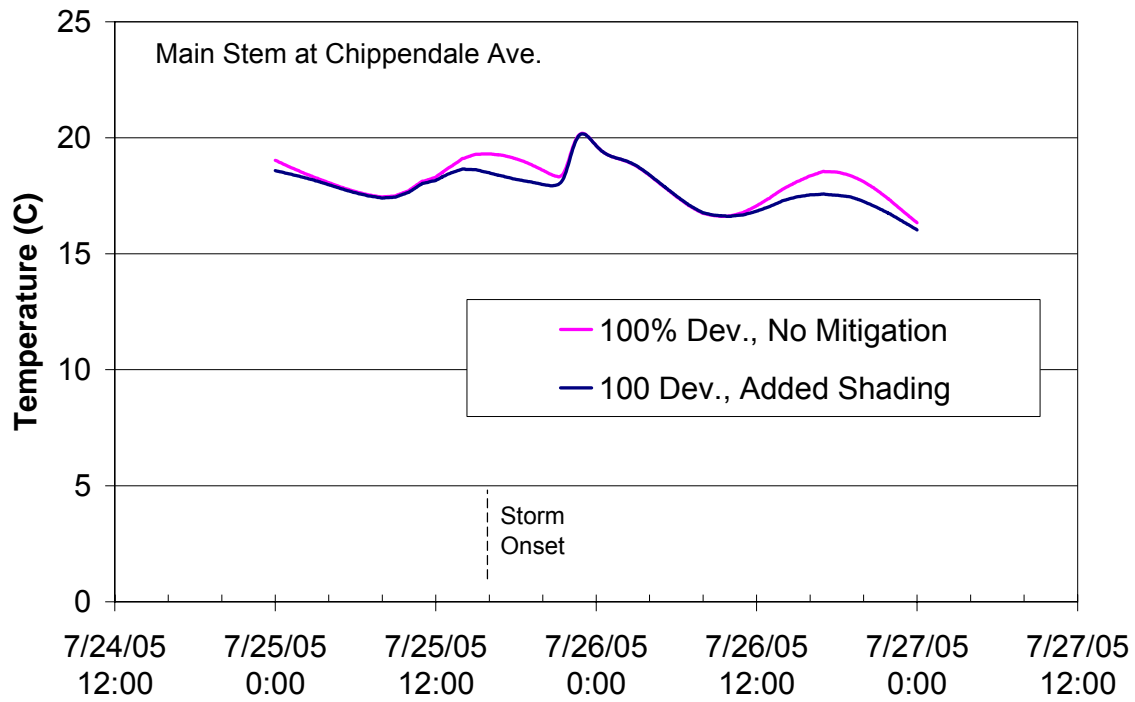


Figure 8.4. Simulated stream temperature time series for the 100% development case, with and without additional stream shading mitigation.

## 9. Summary of Results

In general, the impact of surface runoff on water temperatures in a receiving stream tends to be highest in small, upstream tributaries and decreases with distance downstream. The decrease in impact with downstream distance is caused by 1) heat loss to the atmosphere, 2) dilution of streamflow by groundwater and tributary inflows and 3) increased baseline stream temperature due to greater channel width and reduced shading.

Given sufficient distance and time to cool, surface runoff inputs in the upstream reaches of a stream increase the flow volume and therefore the ability of the stream to absorb heat energy in downstream inflows. As a result, the response of a stream to multiple surface runoff inputs can be complex. The response is not the sum of the responses to single inputs.

Under design storm conditions, the stream temperature model simulated the highest changes in stream temperature just downstream of the pour points, i.e. the points in the stream where surface runoff is introduced. The model pour points do not, in all cases, represent actual locations of surface runoff inputs. It is therefore more appropriate to use reach-averaged temperatures, rather than temperatures at individual nodes, to evaluate the hydrothermal response of a stream to runoff inputs

The stream thermal impact model is able to show the response of the Vermillion River to a new urban development of 200 acres. A measureable change ( $> 0.1^{\circ}\text{C}$  increase) in stream temperature is simulated for several miles in South Creek, a Vermillion River tributary that receives the surface runoff from the development.

The 50% and 100% urban development scenarios on upper South Creek resulted in noticeable changes in stream temperature downstream as far as the Empire WWTP. Increases in maximum stream temperature during the runoff event ranged from  $3.8^{\circ}\text{C}$  in South Creek to  $0.07^{\circ}\text{C}$  for the main stem reach ending at the Empire WWTP discharge. The stream temperature excess duration above  $20^{\circ}\text{C}$  also increased for the 50% and 100% development scenarios, by up to 2.4 hours. The development scenarios did not, in general, cause stream temperature to exceed  $23^{\circ}\text{C}$ , i.e. lethal temperature conditions for trout.

Additional stream shading and wind sheltering did not reduce temperature spikes during the design storm runoff event, because solar heating is not a significant heat source during runoff events. Adding stream shading and wind sheltering did reduce mid-day stream temperatures during dry weather prior to and after the rainfall event, by about  $1^{\circ}\text{C}$ .

Disconnecting commercial roofs from runoff in downstream sub-watersheds gave partial temperature mitigation for the South Creek development scenarios, but available roof area was insufficient for full thermal mitigation. Conversion of agricultural land to wetland in downstream sub-watersheds gave no temperature mitigation of the South Creek development scenarios, because the  $\frac{1}{2}$ " design storm used for the study produced no runoff from either agricultural or wetland land use.

The results in this report are mainly for simulations of a single storm event, i.e. the ½” design storm. Other storm events may give different surface runoff characteristics and stream flow and temperature responses. The ½” design storm should represent an upper bound for runoff temperature; larger volume storms would give larger runoff volumes at lower mean runoff temperatures. The ½” design storm represents an upper bound for thermal impact on small tributaries, since 1) runoff temperatures are high and 2) the runoff volume is sufficient to substantially increase stream flow in small tributaries. A larger volume storm with high dew point temperature could cause more thermal impact on stream temperature, in terms of the total stream length over which stream temperature exceeds 20°C and the duration of exceedance. It is unlikely, however, that larger storms would cause stream temperatures to exceed 23 °C, since mean runoff temperature would likely be less than 23 °C.

### **Implications for Management of Thermal Impact on Streams due to Land Development**

The results of this study suggest that the thermal impact of a surface runoff into a stream is a localized phenomenon: the highest stream temperature changes occur just downstream of the pour point, and then decrease with downstream distance and time. Therefore, the concept of mitigating an upstream thermal impact due to surface runoff into a stream at some distant downstream location is probably difficult to implement. If existing trout reaches are to be preserved in smaller tributaries, thermal impacts probably need to be addressed with local stormwater mitigation strategies.

On the other hand, it may be quite possible to reduce *additional* downstream thermal impacts by changes in land use, or reduce dry weather stream temperatures at downstream locations by increased channel shading. Since downstream reaches tend to be wider, with less effective shading, and have higher baseflow, stream temperature maxima during hot and dry weather are more likely a problem than surface runoff inputs.

Although limited to the simulation of a design storm event, the results of this study suggest that stream temperature excursions due to surface runoff inputs are no more extreme than temperature excursions due to hot, sunny weather. The mitigation study suggests that additional channel shading is a good candidate for mitigating stream temperatures in hot, sunny weather, but that shading is not a good candidate for mitigating stream temperature excursions for surface runoff.

Although there is often an overall decrease of channel shading from upstream to downstream, several reaches of the Vermillion were found to have locally low shading (Figure 7.5), including reaches on the main stem upstream of the South Creek confluence and downstream of the North Creek confluence. Additional atmospheric (solar) heat inputs in these reaches can be expected to affect stream temperatures in the reach and for some distance downstream of the reach – just as heat inputs from surface runoff do. These reaches may be good targets for reductions in stream temperature by additional shading to compensate for either increased development or climate change.



Due to the focus of this study on the EPA-funded thermal impact trading program, the results do not address methods for local mitigation of thermal impacts from new developments. Additional and separate studies are needed, although some valuable results already exist. For example, simulations and measurements of wet detention ponds have shown that they are ineffective for thermal mitigation (Herb et al. 2006), and stormwater infiltration standards are a good starting point for mitigation of surface runoff thermal impacts (Herb 2008c). The development of management strategies will likely require analysis of multiple storm events or continuous analysis of both sunny and wet weather over periods of several months.

## **Acknowledgments**

This study was conducted with support from the Minnesota Pollution Control Agency, St. Paul, Minnesota, with Bruce Wilson as the project officer. Project guidance was also supplied by Kim Chapman, Applied Ecological Services, Inc., and Paul Nelson, Scott County. Surface runoff inputs from the land cover heat contribution model were supplied by Theresa Nelson, Applied Ecological Services, Inc. Stream flow and temperature data were supplied by Travis Bistodeau of the Dakota County SWCD and the USGS. Precipitation data were obtained from Karen Jensen at the Met Council, and the University of Minnesota Rosemount Research and Outreach Center. Stream channel geometry was supplied by Barr Engineering Company. The authors are grateful to these individuals and organizations for their cooperation.

## References

- Applied Ecological Services (2008). Vermillion River Watershed Surface Heat Loading Model - Modeling Methodology. Unpublished report prepared under an EPA Targeted Watershed Grant (#WS 97512701-0) for the Vermillion River Watershed Joint Powers Organization, Apple Valley, MN.
- Edinger, J., D.K. Brady and J.C. Geyer (1974). Heat exchange and transport in the environment. Report No. 14, Electric Power Research Institute, Cooling Water Discharge Research Project (RP-49), Palo Alto, CA, 125 pp.
- Herb, W.R., M. Weiss, O. Mohseni and H.G. Stefan (2006). Hydrothermal Simulation of a Stormwater Detention Pond or Infiltration Basin. Project Report No. 479, St. Anthony Falls Laboratory, University of Minnesota, 34 pp.
- Herb, W.R., B. Janke, O. Mohseni and H.G. Stefan (2007). Estimation of runoff Temperatures and Heat Export from Different Land and Water Surfaces, St. Anthony Falls Laboratory Report 488, 34 pp.
- Herb, W.R. and H.G. Stefan (2008a). Analysis of Vermillion River Stream Flow Data (Dakota and Scott Counties, Minnesota). Project Report No. 514, St. Anthony Falls Laboratory, University of Minnesota, 28 pp.
- Herb, W.R. and H.G. Stefan (2008b). A flow and temperature model for the Vermillion River, Part I: Model development and baseflow conditions. Project Report No. 517, St. Anthony Falls Laboratory, University of Minnesota, 29 pp.
- Herb, W.R. and H.G. Stefan (2008c). Analysis of the effect of stormwater runoff volume regulations on thermal loading to the Vermillion River. Project Report No. 520, St. Anthony Falls Laboratory, University of Minnesota, 34 pp.
- Sinokrot, B.A. and Stefan, H.G. (1993). Stream Temperature Dynamics: Measurements and Modeling, *Water Resources Research* 29(7): 2299-2312.
- Sinokrot, B.A. and Stefan, H.G. (1994). Stream Water Temperature Sensitivity to Weather Parameters, *Jour. Hydraulic Engineering* 120(6): 722-736.
- US ACE (2008). HEC-RAS River Analysis System, version 4.0, U.S. Army Corps of Engineers, Hydrologic Engineering Center, Sacramento, California.  
<http://www.hec.usace.army.mil/software/hec-ras/>.
- US EPA (2005). One-dimensional Riverine Hydrodynamic and Water Quality Model, U.S. Environmental Protection Agency, Athens, Georgia.  
<http://www.epa.gov/ATHENS/wwqtsc/html/epd-riv1.html>.

## Appendix I. Analytic model for temperature decay of surface runoff

This appendix describes several methods for estimating the time variation of surface runoff as it progresses through a drainage network. For relatively short runoff periods, when dew point temperature and solar radiation can be taken as constants, a simple exponential decay model based on a fixed equilibrium temperature may give reasonable results, and can be implemented in a watershed-level runoff analysis. If the period of runoff after a storm includes substantial solar radiation, it may be more difficult to adequately predict the time variation of runoff temperature, and in particular, the runoff temperature as it enters the stream system.

### Equilibrium Temperature

The equilibrium temperature ( $T_e$ ) of a surface water body is defined as the water temperature at which the water body has reached thermal equilibrium with the atmosphere, e.g. zero net heat flux between the water surface and the atmosphere. Equilibrium temperature can be used as the basis to develop simple models to predict the temperature of surface water bodies, e.g. lakes and streams (Edinger et al. 1968, 1974).

Equilibrium temperature depends on climate parameters, including air temperature, humidity, solar radiation, cloud cover, and wind speed. One way to calculate equilibrium temperature (referred to here as Method 1) is to consider the sum of the various heat transfer components between the atmosphere and the surface of a water body, e.g.

$$h_{\text{net}} = h_{\text{rad}} - h_{\text{evap}} - h_{\text{conv}} \quad (\text{A1.1})$$

where  $h_{\text{net}}$  is the total net surface heat transfer,  $h_{\text{rad}}$  is net short and long wave radiation,  $h_{\text{evap}}$  is evaporative heat transfer, and  $h_{\text{conv}}$  is convective (sensible) heat transfer. Further details required to calculate these heat transfer components are given in, e.g., Herb et al. (2006) or Edinger (1974). All three components are functions of both atmospheric parameters and the surface temperature of the water body. Given a set of observed climate parameters, one can solve for a value of surface temperature,  $T_s$ , such that  $h_{\text{net}} = 0$ . This value of  $T_s$  is the equilibrium temperature ( $T_e$ ). This calculation can be performed for relatively short time steps, e.g. hourly, so that  $T_e$  is a dynamic quantity that varies with the specified climate parameters, or for relatively long time steps, e.g. daily or weekly, using averaged climate parameters.

Equilibrium temperature can also be estimated using approximate functions (Edinger et al. 1968, 1974).

$$T_e = T_d + \frac{h_s}{K} \quad (^\circ\text{C}) \quad (\text{A1.2})$$

$$K = 4.5 + 0.05 T_s + (0.47 + \beta)f(W) \quad (\text{W/m}^2/^\circ\text{C}) \quad (\text{A1.3})$$

$$\beta = \frac{e_s - e_a}{T_s - T_a} \quad (\text{mmHg}/^\circ\text{C}) \quad (\text{A1.4})$$

$$f(W) = 9.2 + 0.46 W^2 \text{ (W/m}^2\text{/mmHg)} \quad (\text{A1.5})$$

where  $T_d$  is dew point temperature  $h_s$  is the net solar radiation, and  $K$  is the bulk surface heat transfer coefficient,  $\beta$  is the slope of vapor pressure versus temperature,  $e_s$  and  $e_a$  (mm Hg) are the saturated vapor pressure at  $T_s$  and the atmospheric vapor pressure, respectively,  $W$  is wind speed (m/s), and  $f(W)$  is a wind speed function for the evaporation and convective heat transfer components. Equation A1.5 gives an example of one wind speed function; many others exist (Edinger 1974). Since  $K$  depends on  $T_s$ , it is generally required to iterate the calculation of  $T_e$  several times, replacing  $T_s$  in Equations A1.3 and A1.4 by  $T_e$  during each iteration. We will refer to this approximate method for calculating  $T_e$  as Method 2.

An example of equilibrium temperature calculated using Methods 1 and 2 is given in Figure A1.1, where the calculation has been performed for 15 minute time steps. At night,  $T_e$  is close to dew point temperature, while during the day,  $T_e$  increases significantly above dew point if bright sun is present.

It is useful to note that  $T_e$  can be very dynamic, varying at the temporal scale of climate parameters. We can also calculate equilibrium temperature for longer time periods based on averaged climate parameters, which is commonly done for lakes. Calculated equilibrium temperature values for a nighttime period and for a full 24 hour period are given in Table A1.1.

Table A1.1. Equilibrium temperature calculated using climate data averaged over 12 and 24 hour time periods using Methods 1 and 2. Climate data are shown in Figure 1. Bulk heat transfer coefficient,  $K$ , required for Method 2 (Equation A1.3) is also given.

Time Period	$T_d$ (°C)	$T_e$ (°C)		$K$ (W/m <sup>2</sup> /°C)
		Method 1	Method 2	
7/30/99 18:00 to 7/31/99 06:00	19.6	18.4	19.9	21.6
7/30/99 18:00 to 7/31/99 18:00	17.1	27.7	28.9	27.5

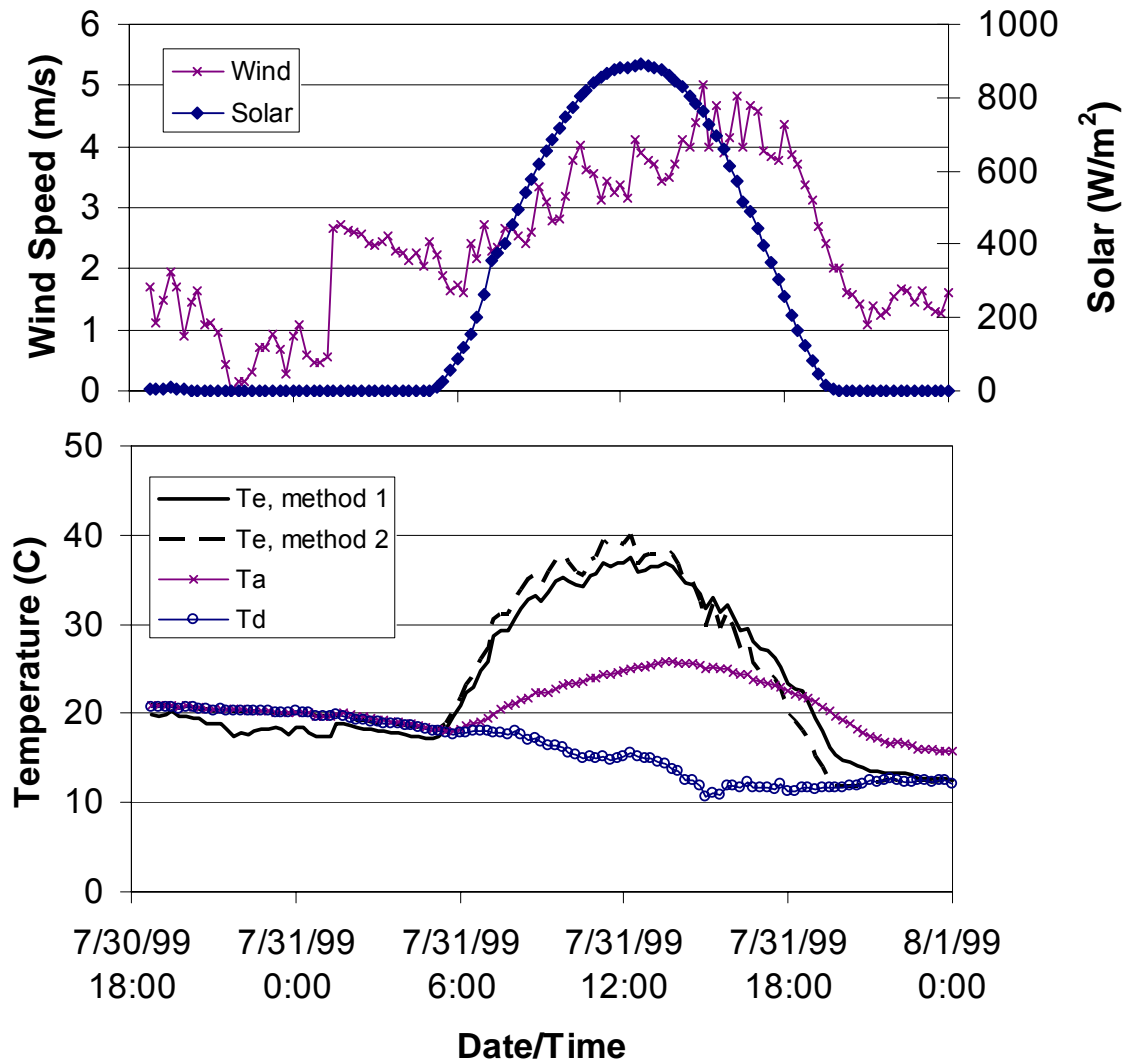


Figure A1.1. Equilibrium temperature calculated by Methods 1 and 2; observed air temperature ( $T_a$ ) and dew point temperature ( $T_d$ ) (lower panel), solar radiation ( $h_s$ ) and wind speed ( $W$ ) (upper panel) used in the calculations. Data are from the MnROAD facility in Albertville, Minnesota. The time series begins after an afternoon rainfall event on July 30, 1999.

### Runoff Temperature Dynamics

Herb et al. (2007) gave results for computed runoff temperatures from small parcels of land assuming that sheet flow dominates the runoff process. The temperatures are calculated considering both atmospheric heat transfer and heat transfer between the runoff and the ground. We now seek ways to estimate changes in water temperature as runoff progress through a drainage network, based on climate conditions after the storm. The “small parcel” runoff temperatures given by Herb et al. (2007) are the initial condition for this analysis.

We can calculate the rate of change of temperature of a parcel of surface water rather directly based on the net surface heat transfer ( $h_{\text{net}}$ ) previously given by Equation A1.1.

$$\frac{dT_s}{dt} = \frac{h_{\text{net}}}{\rho C_p d} \quad (\text{°C/s}) \quad (\text{A1.6})$$

Equation A1.6 estimates the rate of change of temperature of a (moving) well-mixed volume of water of temperature  $T_s$ , i.e. in Lagrangian coordinates. This analysis ignores heat transfer between the runoff and the ground, which can be expected to give relatively minor errors for channelized flow and relatively large errors for sheet flow. As might be expected, a thinner water layer ( $d$ ) will reach equilibrium temperature more quickly.

Based on a calculated equilibrium temperature, the rate of change of surface temperature of a water body can be estimated as (Edinger 1974):

$$\frac{dT_s}{dt} = \frac{K(T_e - T_s)}{\rho C_p d} \quad (\text{°C/s}) \quad (\text{A1.7})$$

where  $\rho$ ,  $C_p$ , and  $d$  are the density, specific heat, and depth of the water layer under consideration, and  $K$  is the bulk heat transfer coefficient (Equation A1.3).

Figure A1.2 compares the time variation of water temperature calculated using Equations A1.6 and A1.7, for three different water depths. Equations A1.6 and A1.7 give very similar results for the case given in Figure A1.2. For the nighttime period,  $T_s$  decreases along with  $T_e$ , with less difference ( $T_s - T_e$ ) for thinner water layers. As  $T_e$  subsequently increases towards mid-day, a lagged response is seen in  $T_s$ , with less time lag and a stronger response for thinner water layers.

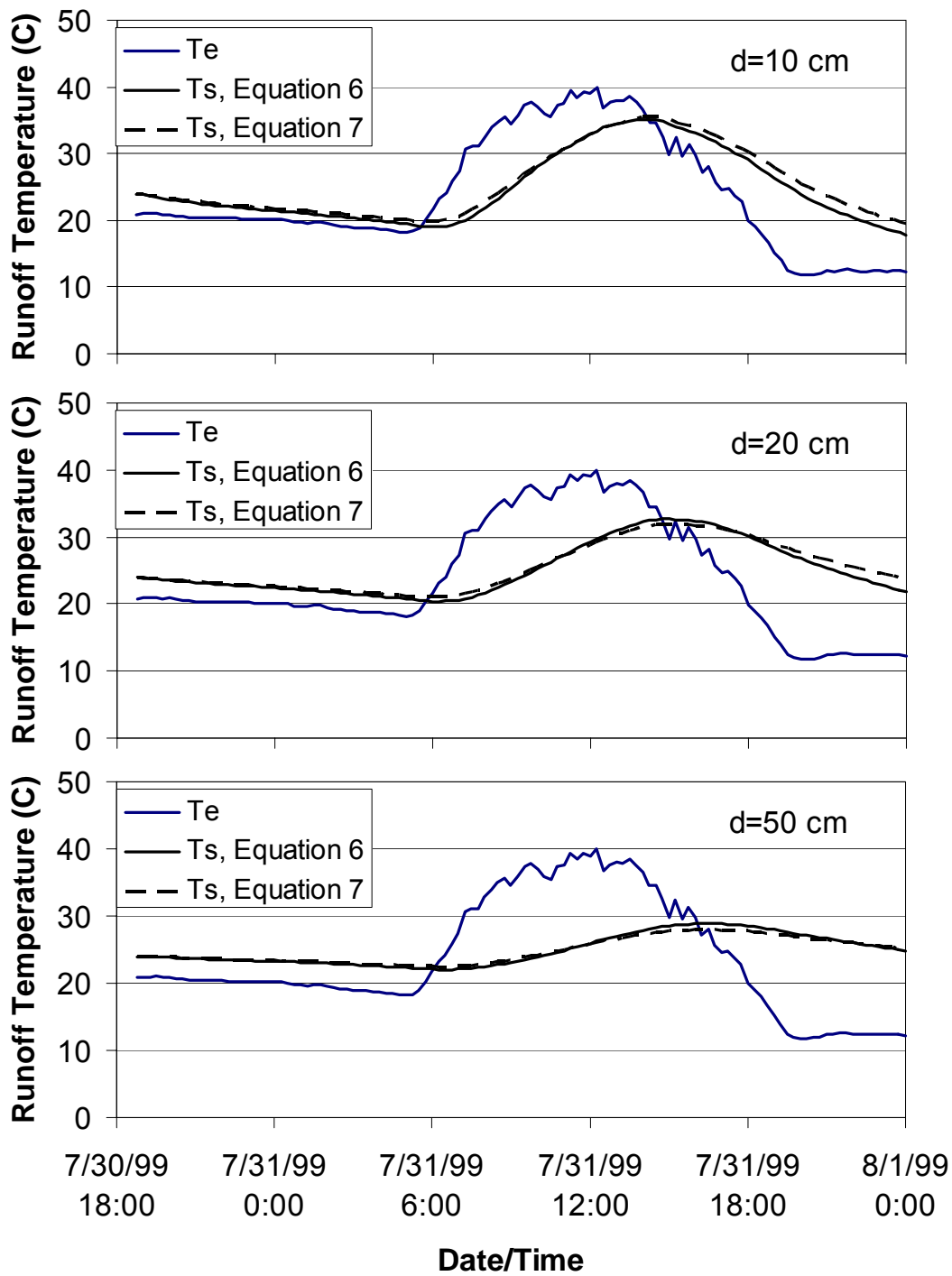


Figure A1.2. Calculated runoff temperature versus time using Equation A1.6 and Equation A1.7 for a 24°C initial runoff temperature and constant runoff depths of 10, 20, and 50 cm.

## Analytic Model for Runoff Temperature Dynamics

Equation A1.6 or A1.7 can be used to predict the time variation of runoff temperature given detailed climate data following a rainfall event. If equilibrium temperature is considered constant over the duration of runoff, an analytic solution can be found for the variation of runoff temperature with travel (flow) time:

$$T_s(t) = T_e + (T_o - T_e) \exp(-t/\tau) \quad (\text{A1.8})$$

where the time constant  $\tau = (\rho C_p d)/K$ ,  $T_o$  is the initial runoff temperature, and  $K$  is the bulk heat transfer coefficient given by Equation A1.3. If, for example, we pick the period of 12 hours (7/30/99 18:00 to 7/31/99 06:00), we can calculate an equilibrium temperature for the period (Equation A1.2, Table A1.1) and a mean value of  $K$  for the period (Equation A1.3). Example results are given in Figure A1.3 in comparison to Equation A1.7 for both 12 hour and 24 hour periods. For the 12 hour period, taking  $T_e$  as a constant is a relatively good assumption, and Equation A1.8 reproduces the results of Equation A1.7 quite well. For the 24 hour period (7/30/99 18:00 to 7/31/99 18:00), taking  $T_e$  as a constant value is a poor assumption (Figure A1.2), and Equation A1.8 does not represent either the time variation over the period of analysis nor the final value (28.9°C) compared to Equation A1.7 (19.5°C).

These results suggest that for relatively short runoff periods, when dew point temperature and solar radiation can be taken as constants, Equation A1.8 may give reasonable results, and will be relatively simple to implement in a watershed-level runoff analysis. If the period of runoff after a storm includes substantial solar radiation, Equation A1.8 may give substantial errors.

The implementation of Equation A1.8 in a watershed-level runoff analysis could proceed as follows:

- 1) The numbers from the “small parcel” runoff analysis are the initial condition for runoff temperature.
- 2) A suitable, average dew point temperature and solar radiation for the post-storm period of runoff is chosen.
- 3) Based on these dew point temperature and solar radiation values, a fixed equilibrium temperature and  $K$  value is estimated for the runoff period.
- 4) Based on the watershed and storm characteristics, an average runoff depth and travel time is estimated.
- 5) Based on the estimate of travel time and runoff depth, the final runoff temperature is calculated using Equation A1.8, which will be somewhere between the initial runoff temperature and equilibrium temperature.



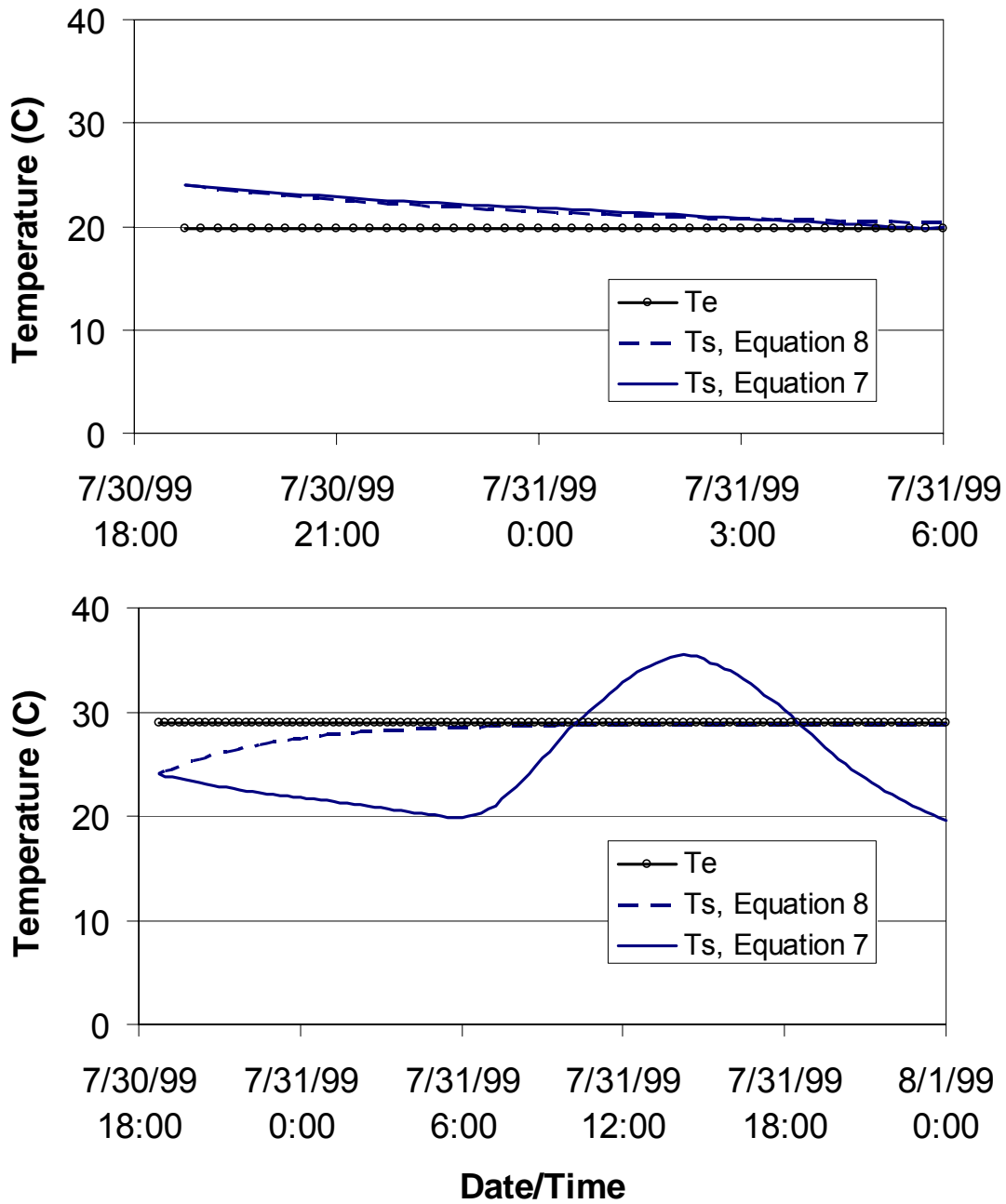


Figure A1.3. Calculated runoff temperature versus time using Equation A1.7 and Equation A1.8 for a 24°C initial runoff temperature and constant runoff depth of 10 cm. In the upper panel,  $T_s$  was calculated over a 12 hour period using Equation A1.8, with  $T_e$  and  $K$  calculated using 12 hour average climate data. In the lower panel,  $T_s$  was calculated over a 24 hour period using Equation A1.8, with  $T_e$  and  $K$  calculated using 24 hour average climate data.

## References

- Edinger, J.E., D.W. Duttweiler and J.C. Geyer. J.C. (1968). The Response of water Temperatures to Meteorological Conditions. *Water Resources Research* 4(5):11337-1145. December 1968.
- Edinger, J.E., Brady, D.K. and Geyer. J.C. (1974). Heat Exchange in the Environment. Report No. 14, Cooling Water Discharge Research Project RP-49, Electric Power Research Institute, Palo Alto, CA, 125 pp.
- Herb, W.R., Janke, B., Mohseni, O., and H.G. Stefan. 2006. All-Weather Ground Surface Temperature Simulation. University of Minnesota, St. Anthony Falls Laboratory Project Report No. 478.
- Herb, W.R., Janke, B., Mohseni, O., and H.G. Stefan. 2007. Estimation of Runoff Temperatures and Heat Export from Different Land and Water Surfaces. University of Minnesota, St. Anthony Falls Laboratory Project Report No. 488.

## **Appendix II. Design storm**

Selection of a design storm began with analyses of six years of simulated runoff data from different land uses, based on observed climate data from the MnROAD facility in Albertville, MN (Herb et al. 2007). Based on cluster analyses performed by Applied Ecological Services, a set of 13 observed storm events was selected that gave high heat export from paved surfaces. These storms are listed in Table A2.1. The rainfall amount for the design storm (1.29 cm, 0.51 in) was determined from the average of these 13 storms. To determine the temporal distribution of rainfall during the design storm, the rainfall patterns from 2 of the 13 observed storms with similar duration to the design storm (2 hours) were averaged. The antecedent conditions were determined by averaging the conditions for all 13 storms. The design storm was then inserted into a 2005 climate time series for the Vermillion River watershed on July 25, replacing an observed precipitation event. The climate time series for the design storm are given in Figure A2.1.

### **References**

Herb, W.R., Janke, B., Mohseni, O., and H.G. Stefan. 2007. Estimation of Runoff Temperatures and Heat Export from Different Land and Water Surfaces. University of Minnesota, St. Anthony Falls Lab Project Report No. 488.

Table A2.1. Summary of the 13 observed storm events used to create the design storm.

Storm No.	Start Date/Time	Duration (hours)	Total Rain (cm)	Total Runoff (cm)	Average for 1 hour prior to event				
					Air Temp (C)	Dew Point (C)	Wind (m/s)	Solar (W/m <sup>2</sup> )	Surface Temp (C)
1	6/26/98 16:30	1.00	0.74	0.71	27.6	19.8	4.0	271.6	42.5
2	8/5/98 17:15	4.00	1.22	1.13	24.2	17.7	2.3	151.0	37.9
3	6/22/99 15:14	5.75	1.46	1.27	27.8	19.9	5.3	421.2	40.1
4	7/30/99 15:45	3.75	2.06	1.97	30.3	24.9	2.9	10.5	39.3
5	6/20/00 17:15	0.75	0.41	0.39	22.9	12.9	3.5	328.4	35.3
6	6/28/03 14:30	1.00	0.66	0.61	23.4	15.9	0.9	618.2	54.4
7	7/11/03 13:15	1.00	0.28	0.22	23.7	16.0	3.9	658.2	43.4
8	7/31/03 15:45	2.00	0.77	0.68	25.0	18.1	1.2	269.3	47.5
9	8/25/04 16:44	3.00	2.96	2.95	25.0	22.7	0.5	56.1	39.2
10	6/20/05 11:30	2.25	3.82	3.76	24.2	19.1	2.1	409.9	46.1
11	7/25/05 15:14	3.25	1.10	1.06	26.0	20.0	0.7	66.7	39.7
12	8/9/05 12:45	0.75	0.21	0.18	25.7	19.0	0.7	295.2	42.2
13	8/16/05 16:30	0.75	1.12	1.10	28.1	16.9	2.5	411.2	48.7
<b>Mean</b>		<b>2.25</b>	<b>1.29</b>	<b>1.23</b>	<b>25.68</b>	<b>18.68</b>	<b>2.34</b>	<b>305.20</b>	<b>42.79</b>

Storm No.	Average value during event					Total Heat Export (kJ/m <sup>2</sup> )	Average Heat Export Rate (W/m <sup>2</sup> )
	Air Temp (C)	Dew Point (C)	Wind (m/s)	Solar (W/m <sup>2</sup> )	Runoff Temp (C)		
1	24.4	20.2	3.4	4.6	27.2	275.2	76.4
2	19.3	18.1	1.1	28.6	23.2	246.0	17.1
3	21.2	20.0	3.9	25.6	26.2	434.7	21.0
4	21.2	20.7	2.7	3.7	22.3	355.0	26.3
5	19.3	14.8	2.3	243.5	28.2	166.5	61.7
6	17.2	13.5	2.1	65.2	31.4	341.4	94.8
7	18.1	16.2	3.0	131.7	34.8	157.3	43.7
8	19.5	18.4	1.3	79.4	31.5	384.6	53.4
9	18.4	18.9	1.7	1.4	22.7	585.3	54.2
10	18.5	18.3	2.7	6.3	23.4	855.4	105.6
11	19.2	17.9	2.0	15.8	21.4	150.6	12.9
12	22.4	19.8	1.1	122.9	36.2	141.0	52.2
13	19.1	16.6	1.6	164.8	33.0	691.9	256.3
<b>Mean</b>	<b>19.82</b>	<b>17.96</b>	<b>2.21</b>	<b>68.74</b>	<b>27.81</b>	<b>368.07</b>	<b>67.35</b>

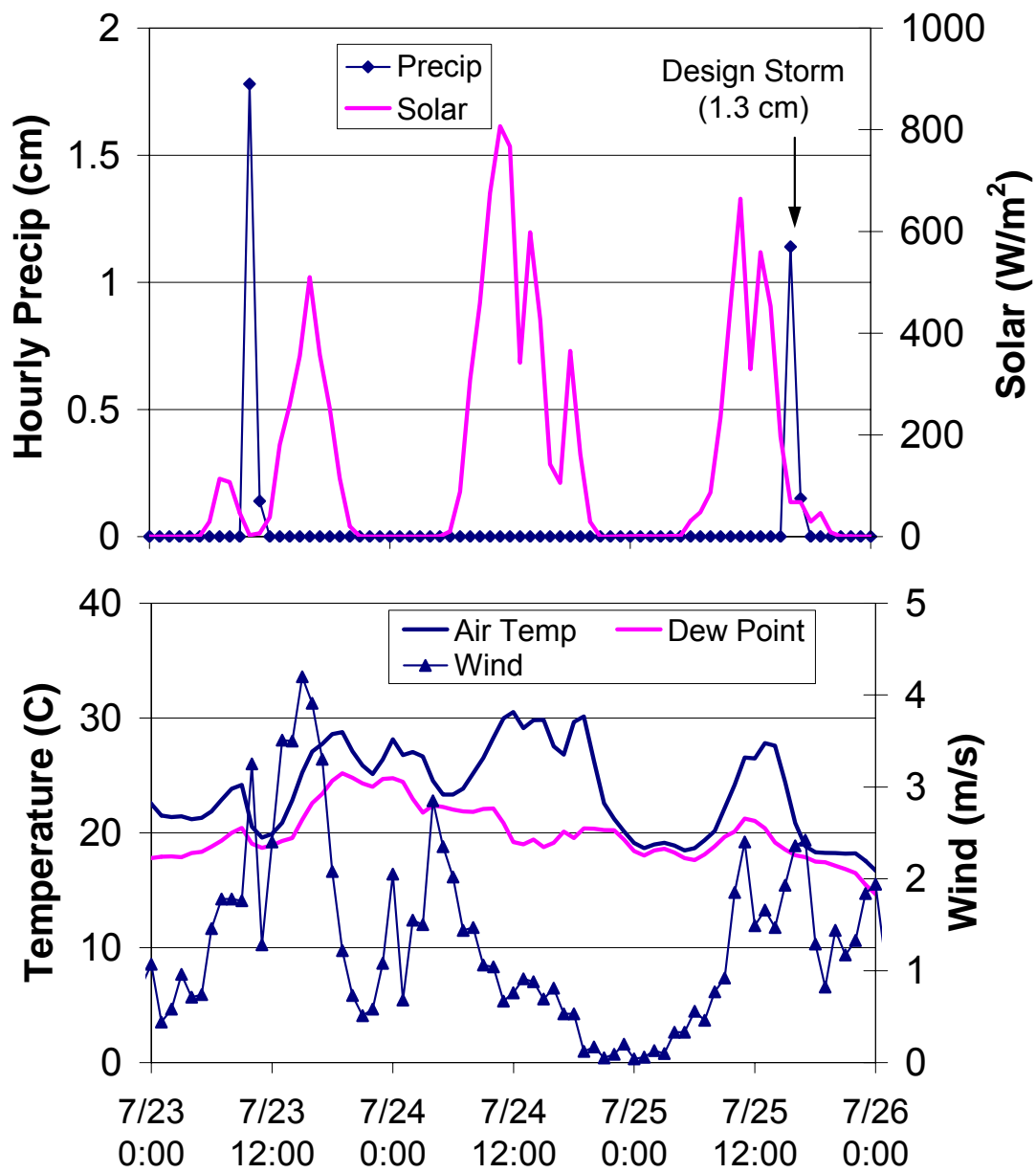


Figure A2.1. Time series of air temperature, dew point temperature, wind speed, solar radiation, and precipitation.